nature genetics

Article

https://doi.org/10.1038/s41588-025-02269-0

Uncovering the multivariate genetic architecture of frailty with genomic structural equation modeling

Received: 30 July 2024

Accepted: 18 June 2025

Published online: 04 August 2025

Check for updates

Isabelle F. Foote[1,2] ✉, Jonny P. Flint[3,4,5,6,7], Anna E. Fürtjes[3,4], Jeremy M. Lawrence[1,8], Donncha S. Mullin[7,9], John D. Fisk[10,11], Tobias K. Karakach[12], Andrew Rutenberg[13], Nicholas G. Martin[6], Michelle K. Lupton[6,14,15], David J. Llewellyn[16,17], Janice M. Ranson[16], Simon R. Cox[3,4], Michelle Luciano[3,4], Kenneth Rockwood[10,11] & Andrew D. Grotzinger[1,8]

Frailty is a multifaceted clinical state associated with accelerated aging and adverse health outcomes. Informed etiological models of frailty hold promise for producing widespread health improvements across the aging population. Frailty is currently measured using aggregate scores, which obscure etiological pathways that are only relevant to subcomponents of frailty. Here we perform a multivariate genome-wide association study of the latent genetic architecture between 30 frailty deficits, which identifies 408 genomic risk loci. Our model includes a general factor of genetic overlap across all deficits, plus six new factors indexing a shared genetic signal across specific groups of deficits. We demonstrate the added clinical and etiological value of the six factors, including predicting frailty in external datasets, highlighting divergent genetic correlations with clinically relevant outcomes and uncovering unique underlying biology linked to aging. We show that nuanced models of frailty are key to understanding its causes and how it relates to worse health.

Frailty is a complex clinical state that affects more than 40% of adults aged over 65 years[1]. It is defined as a state of progressive, multisystem physiological decline that reduces an individual's ability to withstand external stressors[1]. This deterioration can lead to both physical and mental impairments and is strongly associated with adverse health outcomes, including earlier mortality[2] and increased levels of disability and hospitalization[3]. Global population aging means that frailty represents a growing public health concern[4]. Family-based studies indicate a substantial genetic component to frailty, with heritability estimates of ~45% (ref. 5). Therefore, genetic methods offer a promising tool to better understand the risk pathways to this critical health state. Nevertheless, the etiology of frailty is largely unknown, limiting our potential to identify effective therapeutic or preventive treatments. We hypothesized that what has limited our etiological understanding is that we have traditionally only considered aggregate measurements of frailty in genetic studies.

The two most common methods for measuring frailty are the Frailty Index (FI) and the Fried Frailty Phenotype (FP)[6,7]. The FI quantifies frailty by calculating the proportion of 'deficits' that are present in an individual from a set of 30 or more phenotypes associated with poor health outcomes in older adults[6]. The FP uses an aggregate score across five physical frailty deficits (weight loss, weakness, exhaustion, slow walking speed and physical inactivity), where the presence of three or more of these deficits indicates frailty[7]. Although the FP has been widely reported in large samples, it is intended to capture pathways of physical frailty and may not provide sufficient information to assess

A full list of affiliations appears at the end of the paper. ✉e-mail: isabelle.foote@colorado.edu

https://doi.org/10.1038/s41588-025-02269-0

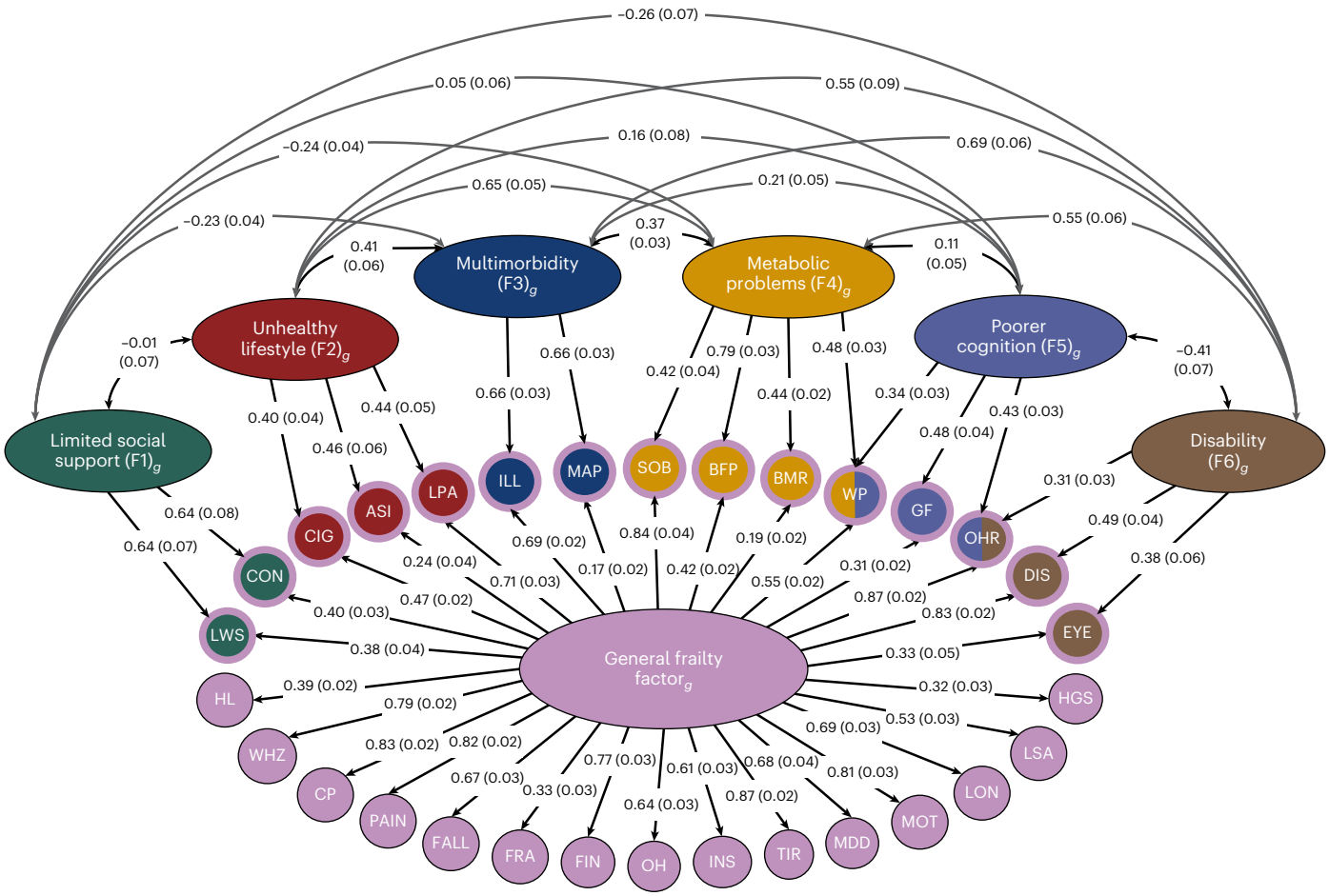

Fig. 1 | Path diagram of the standardized results for our bifactor model of frailty. All 30 frailty deficits load onto the general factor of frailty (large oval), which is orthogonal to factors 1–6 (that is, residual factors). The small circles represent the 30 measured frailty indicators (that is, genetic variance captured in the univariate GWAS for that phenotype), whereas the medium-size ovals represent latent factors (that is, unmeasured constructs representing genetic overlap (*g*) between the indicators that load onto them). Single-headed arrows represent a directional genetic correlation between a latent factor and an indicator (that is, factor loadings), whereas curved double-headed arrows represent inter-factor correlations between factors 1 to 6; the s.e. of the correlation coefficients is reported in the parentheses. ASI, pulse wave arterial stiffness index; BFP, body fat percentage; BMR, basal metabolic rate; CIG, number of cigarettes smoked per day; CON, unable to confide; CP, chest pain; DIS, long-standing illness, disability or infirmity; EYE, eye disorder or problem; FALL, number of falls in past year; FIN, financial difficulties; FRA, fracture in last 5 years; GF, low fluid intelligence score; HGS, low hand grip strength; HL, age-related hearing loss; ILL, number of non-cancer illnesses; INS, insomnia; LON, loneliness or isolation; LPA, physical inactivity; LSA, low social or leisure activity; LWS, not living with spouse or partner; MAP, mean arterial pressure; MDD, major depressive disorder; MOT, feelings of unenthusiasm or disinterest; OH, poor oral health; OHR, poorer overall health rating; PAIN, pain experienced in the past month; SOB, shortness of breath when walking on flat ground; TIR, tiredness or lethargy; WHZ, wheezing or whistling in chest in the past year; WP, slow walking pace.

the more nuanced subgroupings that may occur in the broader frailty construct[8]. By contrast, the deficits that form the FI span many levels of functional, psychological and social aspects of health, allowing frailty to be measured across a broad spectrum of traits. These FI deficits are heterogeneous and vary in their underlying etiology.

Phenotypic work clearly indicates that the deficits included in the FI are not always strongly correlated and are driven by diverse biological mechanisms[9–11]. Therefore, their combination into a single aggregate score is likely to obscure causal pathways of frailty. For example, previous work that applied principal component (PC) analysis to phenotypic data of FI deficits demonstrated that additional informative variance associated with frailty was captured when three clusters were modeled instead of one cluster[12]. Information that is lost through aggregation could be identified by a more detailed genetic analysis. Recent advances in multivariate genomics, such as the development of genomic structural equation modeling (SEM)[13], offer the opportunity to model the genetic basis of frailty at a multidimensional level.

We used genomic SEM to identify new groupings of genetic overlap between 30 frailty deficits using publicly available genome-wide association study (GWAS) summary statistics. We identified 7 distinct latent factors underpinning frailty, which displayed unique genetic overlap with clinically relevant health outcomes and were defined by divergent sets of genomic risk loci and biological pathways, which provided empirical support for most of the 12 hallmarks of aging[14]. In combination, these latent constructs yielded enhanced prediction of frailty status in external cohorts and a dramatic improvement in genomic locus discovery compared to aggregate measures.

Results

Multivariate genetic architecture of frailty

After careful quality control and selection of frailty deficits from an initial pool of 52 traits (Methods and Supplementary Note), we used genomic SEM to model the genome-wide genetic overlap from GWAS data for 30 frailty deficits[15–19] (Fig. 1 and Supplementary Tables 1 and 2). We provide a detailed explanation of the reasons for the removal of

22 deficits in the Supplementary Note. As genomic SEM can model genetic overlap across participant samples with varying and unknown levels of participant sample overlap, including even mutually exclusive participant samples, this allowed us to bring together the most well-powered genomic studies currently available for the 30 frailty deficits and produce estimates with the highest possible precision. Using a combination of exploratory and confirmatory factor analysis (CFA) (Methods), this modeling procedure yielded a bifactor model that provided a good fit to the data (comparative fit index (CFI) = 0.93; standardized root mean squared residual (SRMR) = 0.07; Fig. 1 and Supplementary Table 3). This model included a general factor that indexed genetic overlap across all 30 deficits; therefore, it is conceptually similar to prior aggregate measures of frailty. Half of the frailty deficits only loaded on the general factor, indicating that the frailty-relevant genetic variance for these deficits was sufficiently captured by a single aggregate factor. The fact that these deficits only loaded on the general factor is conceptually consistent with the broad psychological processes (for example, insomnia, lack of motivation or apathy, loneliness) and general aging-related outcomes (for example, age-related hearing loss, wheezing, pain) that they surveyed.

In addition, the model produced six residual group factors that were orthogonal (that is, uncorrelated) to the general factor, which were defined according to additional genetic overlap in subsets of frailty deficits. These six factors captured distinct, albeit intercorrelated, frailty pathways related to limited social support (factor 1), unhealthy lifestyle (factor 2), multimorbidity (factor 3), metabolic problems (factor 4), poorer cognition (factor 5) and disability (factor 6). We named these residual latent factors according to the frailty deficits that loaded onto them to provide a preliminary interpretation of what each latent factor might be representing (see the Supplementary Note for a description of this factor-naming procedure). These should not be interpreted as definitive descriptions of the pathways underlying them because there may be additional pathways related to that label that are captured by the general factor of frailty or by the unique (residual) variances of the individual frailty deficits.

Our remaining analyses sought to explore the risk pathways underpinning these six residual factors and evaluate their divergent validity and clinical utility by examining their ability to uniquely capture frailty-relevant pathways at increasingly granular levels of biological analysis.

Genetic overlap between frailty and aging-related outcomes

To validate whether the latent factors in the bifactor model reflected different aspects of frailty, we measured the level of genetic correlation (r_g) between each of the latent factors and 52 aging-related health outcomes and established frailty measures (Fig. 2 and Supplementary Tables 4 and 5). All P values were adjusted using false discovery rate (FDR) correction to account for multiple testing (herein provided as q-values). The general factor displayed highly positive genetic correlations with the FI ($r_g = 0.93$, s.e. = 0.02, $q = 9.1 \times 10^{-298}$) and FP ($r_g = 0.83$ (0.02), $q = 9.1 \times 10^{-298}$), indicating that the general factor closely approximates both of these frailty phenotypes, in line with expectations, given that this latent factor represents genetic overlap between all 30 included deficits. These findings were corroborated by the fact that all the latent factors except for factor 1 (limited social support) were associated with shorter parental lifespan ($r_g < -0.31$, $q < 3.2 \times 10^{-6}$), reduced longevity ($r_g < -0.21$, $q < 0.01$), increased risk of common aging-related infections ($r_g > 0.22$, $q < 0.01$), hospitalization because of infection ($r_g > 0.15$, $q < 0.008$) and heart failure ($r_g > 0.15$, $q < 0.005$), all of which reflect key clinical correlates of frailty.

Importantly, our findings support the inclusion of additional subgroups when measuring frailty accumulation by highlighting divergent genetic correlations with aging-related health outcomes. For example, factor 5 (poorer cognition) was the only latent factor to demonstrate positive genetic correlations with Alzheimer's disease ($r_g = 0.32$, s.e. = 0.07, $q = 2.26 \times 10^{-5}$) and amyotrophic lateral sclerosis ($r_g = 0.38$ (0.06), $q = 1.07 \times 10^{-8}$). Factor 5 also captured genetic variance associated with smaller gray matter volume ($r_g = -0.34$ (0.05), $q = 9.53 \times 10^{-12}$) and lacunar stroke ($r_g = 0.25$ (0.09), $q = 9.80 \times 10^{-3}$). By contrast, factor 2 (unhealthy lifestyle) demonstrated genetic correlations with brain-related vascular changes, including increased white matter hyperintensities ($r_g = 0.21$ (0.09), $q = 0.04$) and resting state fluctuation amplitudes ($r_g = 0.19$ (0.08), $q = 0.03$), whereas factor 3 (multimorbidity) was correlated with ischemic and lacunar stroke ($r_g = 0.45$ (0.05), $q = 6.21 \times 10^{-18}$ and $r_g = 0.38$ (0.09), $q = 3.00 \times 10^{-3}$), but not cerebrovascular markers. Finally, all the latent frailty factors displayed distinct patterns of genetic correlations with routinely collected blood and urinary biomarkers (Fig. 2), which may represent potential endophenotype profiles for these frailty subgroups. By definition, the identified relationships are independent of shared risk pathways captured by the general factor of frailty. It follows that our model of frailty has potential clinical utility for targeted prevention and therapeutic intervention in patients who present with elevated risk in a subgroup of frailty deficits.

Multivariate GWAS identifies 408 risk loci for frailty

We subsequently performed a multivariate GWAS of our frailty bifactor model using genomic SEM to uncover genomic risk loci that were associated with each latent frailty factor ($P_{Bonferroni} < 7.14 \times 10^{-9}$). We pruned out any significantly heterogenous genetic signal (Q_{SNP}) from our GWAS results to ensure that we were only measuring genetic effects that were shared between the deficits that defined that particular latent factor (Methods). From this shared signal, we identified a total of 408 genomic risk loci across the seven latent frailty factors (Fig. 3 and Supplementary Tables 6–12). We compared results from our GWAS to the risk loci identified in previously published GWAS of FI[20] (Supplementary Table 13) and FP[21] (Supplementary Table 14). We regarded a locus as being fully replicated if the locus from the original GWAS study (defined as the genomic risk locus ± 100 kb) overlapped with a genomic risk locus in any of the latent factors ($P_{GWAS} < 5 \times 10^{-8}$) or partially replicated if it demonstrated a nominally significant association with one of the latent factors ($P_{Bonferroni} < 0.001$ (that is, 0.05/47)). All the tested loci were replicated by at least one of our latent factors, ensuring that the direction of effect was also concordant across studies when aligned to the same reference allele (Supplementary Tables 13 and 14). We validated six of the FI loci and 21 of the FP loci with the residual factors (that is, factors 1–6) instead of the general factor, indicating that our model can comprehensively define subgroups within the frailty construct, which one aggregate measure overlooks. Furthermore, five of the FI loci and 15 of the FP loci were also significant for the single-nucleotide polymorphism (SNP)-level heterogeneity metric in the current analyses. As Q_{SNP} identifies SNPs that are probably deficit-specific or that show heterogeneous effects between the included frailty deficits, these findings indicate that existing aggregate frailty measures are sensitive to large effects driven by a single indicator that are not part of more general frailty pathways.

Frailty-associated gene expression and epigenetic changes

We completed a series of post-GWAS analyses to explore how the genetics underpinning each of the frailty latent factors may influence the underlying biology. We applied multi-marker analysis of genomic annotation (MAGMA) gene property analysis to test for enriched gene expression changes in 54 body tissues and stratified genomic SEM to test for enrichment in 146 functional annotations linked to gene expression and epigenetic changes in tissues and cell subtypes in the brain (Fig. 4 and Methods).

MAGMA gene property analysis showed significant enrichment in the brain and pituitary gland for all the latent frailty factors except for those underlying the multimorbidity (factor 3) and disability (factor 6) pathways (Fig. 4a). The only other tissues that demonstrated

https://doi.org/10.1038/s41588-025-02269-0

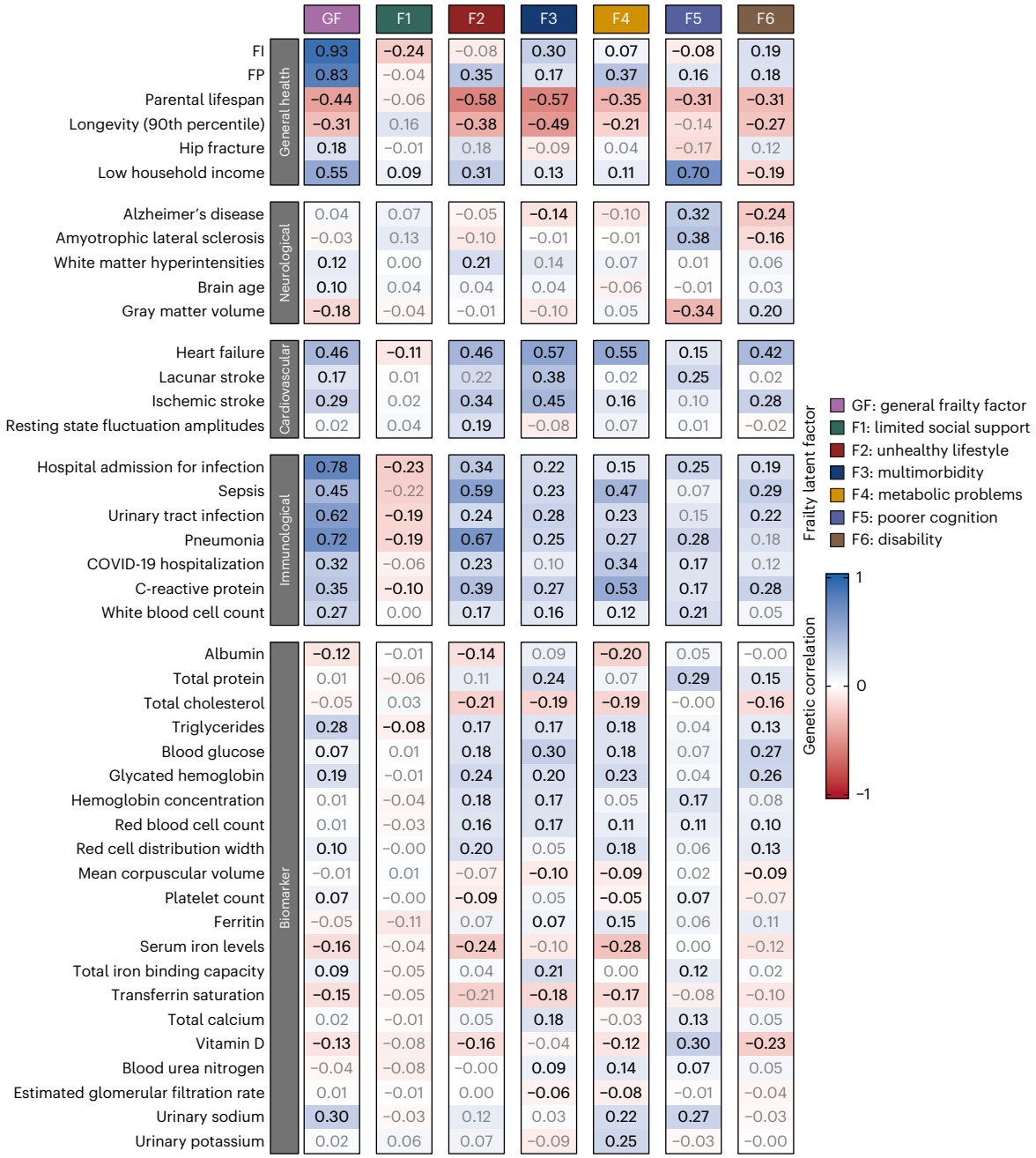

Fig. 2 | Heatmap of the genetic correlations between aging-related health outcomes and each of the latent factors from the frailty bifactor model. Genetic correlations with a two-sided $q < 0.05$ are in black font. We used FDR correction to account for multiple testing. The blue shading represents a positive genetic correlation, whereas the red shading represents a negative genetic correlation. For visualization purposes, only health outcomes that demonstrated at least one $q < 0.05$ with one or more of the latent factors are included in this figure (full results can be found in Supplementary Table 5).

significantly enriched changes in gene expression were the reproductive organs, whereby factor 2 (unhealthy lifestyle) showed significant gene expression changes in the testis, factor 3 (multimorbidity) showed significant changes in gene expression in the cervix and uterus, and factor 5 (poorer cognition) showed significant gene expression changes in the ovaries (Supplementary Table 15).

Stratified genomic SEM provided a more in-depth picture of enrichment in the brain (Supplementary Table 16). We found widespread enrichment in gene expression and epigenetic changes throughout brain regions in oligodendrocytes and neurons for the general factor of frailty. However, the widespread nature of this enrichment demonstrates that using an aggregate measure of frailty is less likely to provide a fine-tuned picture of the underlying mechanisms of frailty because of its generalized impact on brain function. In contrast, residual factors provided a more detailed understanding of the pathways implicated by different frailty deficits, which could present future therapeutic targets within the broad spectrum of frailty (Fig. 4b). For instance, factor 1 (limited social support) only showed significant gene expression changes in the dorsal striatum (caudate and putamen) and methylation changes in the substantia nigra, whereas factor 2 (unhealthy lifestyle) showed enriched gene expression in the spinal cord but not any of the tested brain regions. In addition, factor 5 (poorer cognition) showed gene expression enrichment in excitatory prefrontal cortex neurons and oligodendrocyte precursor cells, as well as epigenetic changes in the angular gyrus, cingulate gyrus, anterior caudate, dorsolateral prefrontal cortex, hippocampus and substantia nigra.

https://doi.org/10.1038/s41588-025-02269-0

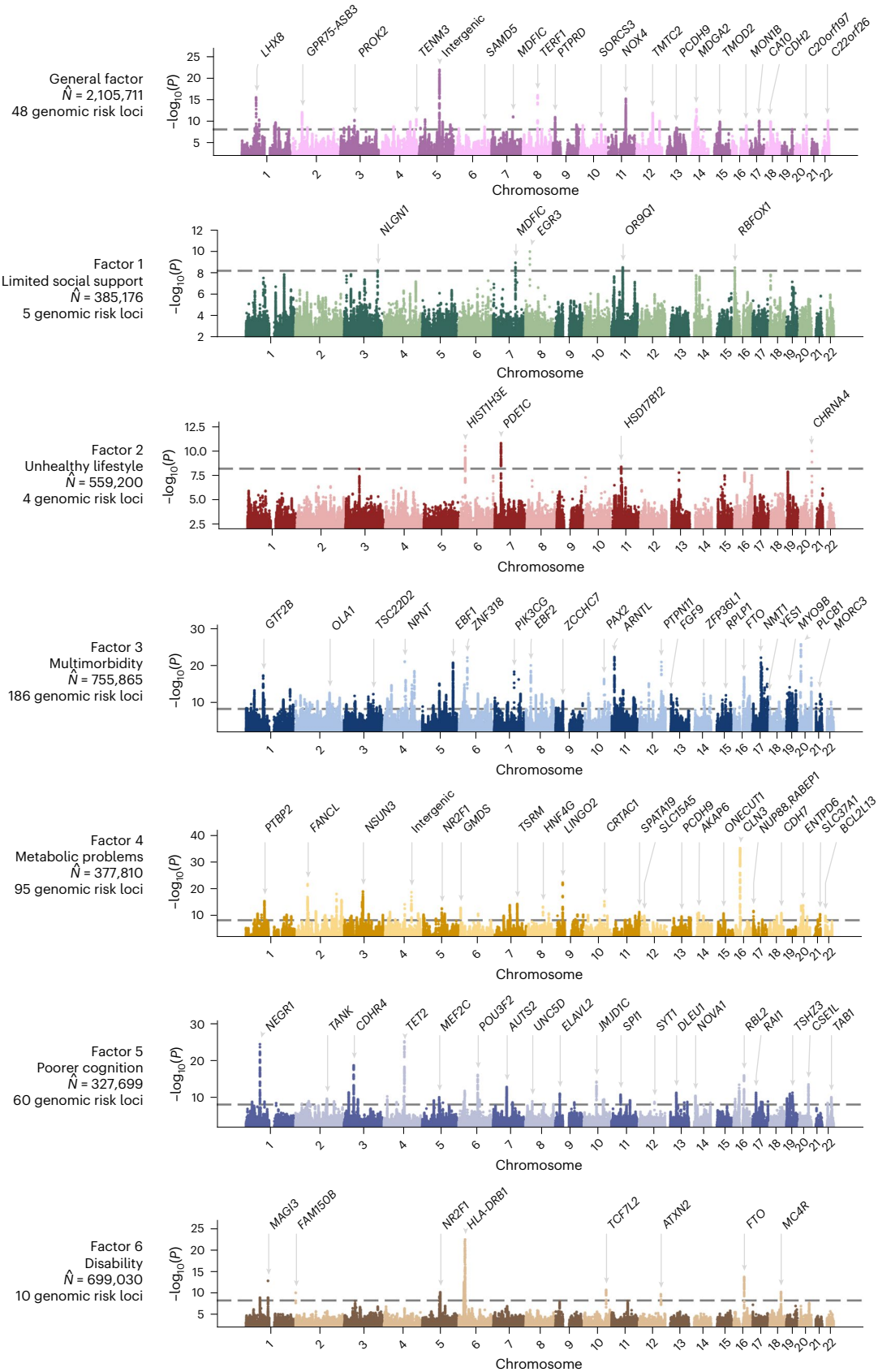

Fig. 3 | Manhattan plots of the shared genetic signal for each of the latent factors in the frailty model. The *x* axis depicts the chromosomes and the *y* axis represents the two-sided $-\log_{10}(P)$ of the association between each individual SNP and each latent factor. The closest gene to the lead SNP is annotated for the top loci of each latent factor. The dashed line denotes the genome-wide significance threshold adjusted for multiple testing using Bonferroni correction (that is, $P_{\text{Bonferroni}} < 7.14 \times 10^{-9}$). $\hat{N}$ is the expected sample size of each latent factor implied by the GWAS summary statistics for that factor, which is influenced by the power of the factor loadings of the indicators (that is, frailty deficits) that define it.

https://doi.org/10.1038/s41588-025-02269-0

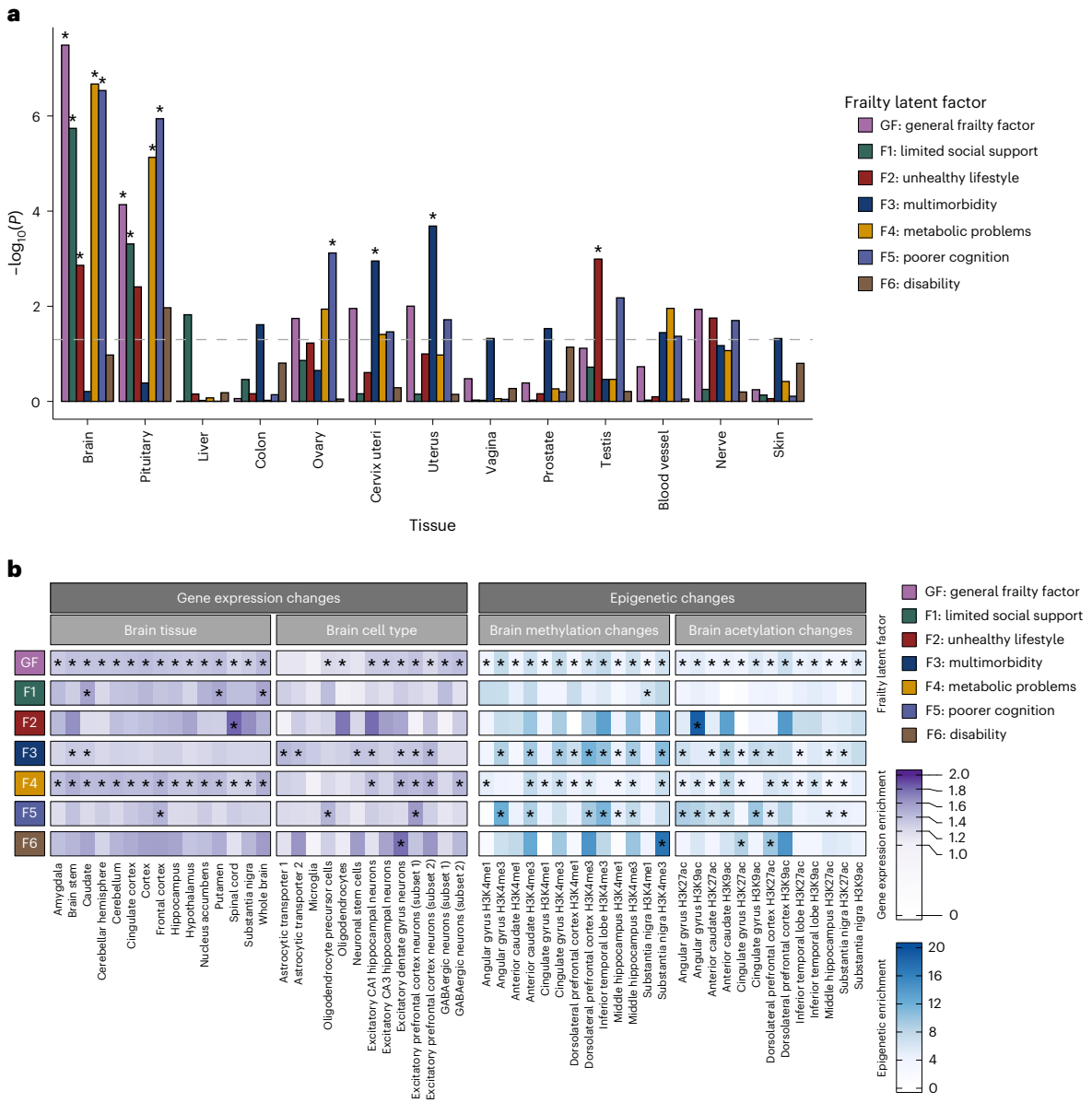

Fig. 4 | Results from the MAGMA gene property analysis and stratified genomic SEM. a, The *y* axis denotes the one-sided $-\log_{10}(P)$ of the enrichment between each latent frailty factor and body tissues from GTEx v.8 (only tissues with significant enrichment are displayed). The dashed line denotes the cutoff for nominal significance (that is, one-sided $P < 0.05$); the bars marked with an asterisk indicate tissues that remained significantly enriched with the latent frailty factor after adjusting for multiple testing using FDR correction (that is, one-sided $q < 0.05$). The full results are shown in Supplementary Table 15. **b**, Heatmaps of the enrichment values calculated using stratified genomic SEM to test for differences in gene expression and epigenetic marks associated with each latent frailty factor in a selection of brain-relevant tissues and cell types. Significant enrichment values that passed FDR correction for multiple testing are marked with an asterisk (that is, one-sided $q < 0.05$). Full results can be found in Supplementary Table 16.

Gene prioritization and pathway analysis

We used five methods to map potentially causal genes to each latent frailty factor to assess the biological pathways that might be associated with each frailty subgroup (Fig. 5a). These methods included mapping SNPs to genes based on their position, whether they were known expression quantitative trait loci (eQTLs) or if they were located in promoter regions known to regulate chromatin interactions (Supplementary Tables 17–23). In addition, we performed a genome-wide gene-based test using MAGMA (Supplementary Tables 24–30) and applied summary-data-based Mendelian randomization (SMR) to identify SNPs that demonstrated evidence of having a pleiotropic effect on expression, splicing or methylation changes in gene function (Supplementary Tables 31–37). We triangulated the results from these five gene mapping techniques and prioritized the most likely candidate genes based on whether they were mapped by three or more of the methods. This resulted in 1,195 genes being prioritized, which we took forward for pathway analysis (54 for the general factor; four for factor 1 (limited social support); 20 for factor 2 (unhealthy lifestyle); 585 for factor 3 (multimorbidity); 194 for factor 4 (metabolic problems); 266 for factor 5 (poorer cognition) and 72 for factor 6 (disability); Supplementary Note). Using METASCAPE, we performed enrichment analysis to identify Gene Ontology and disease pathways that were significantly associated with the prioritized genes mapped to each latent factor[22]. As there can be extensive redundancy between gene sets, we combined highly correlated enriched pathways into clusters, named according to the Gene Ontology pathway that had the strongest enrichment with the latent frailty factors (Methods and Fig. 5b). As the general factor was orthogonal to the other latent frailty factors, we conducted pathway

https://doi.org/10.1038/s41588-025-02269-0

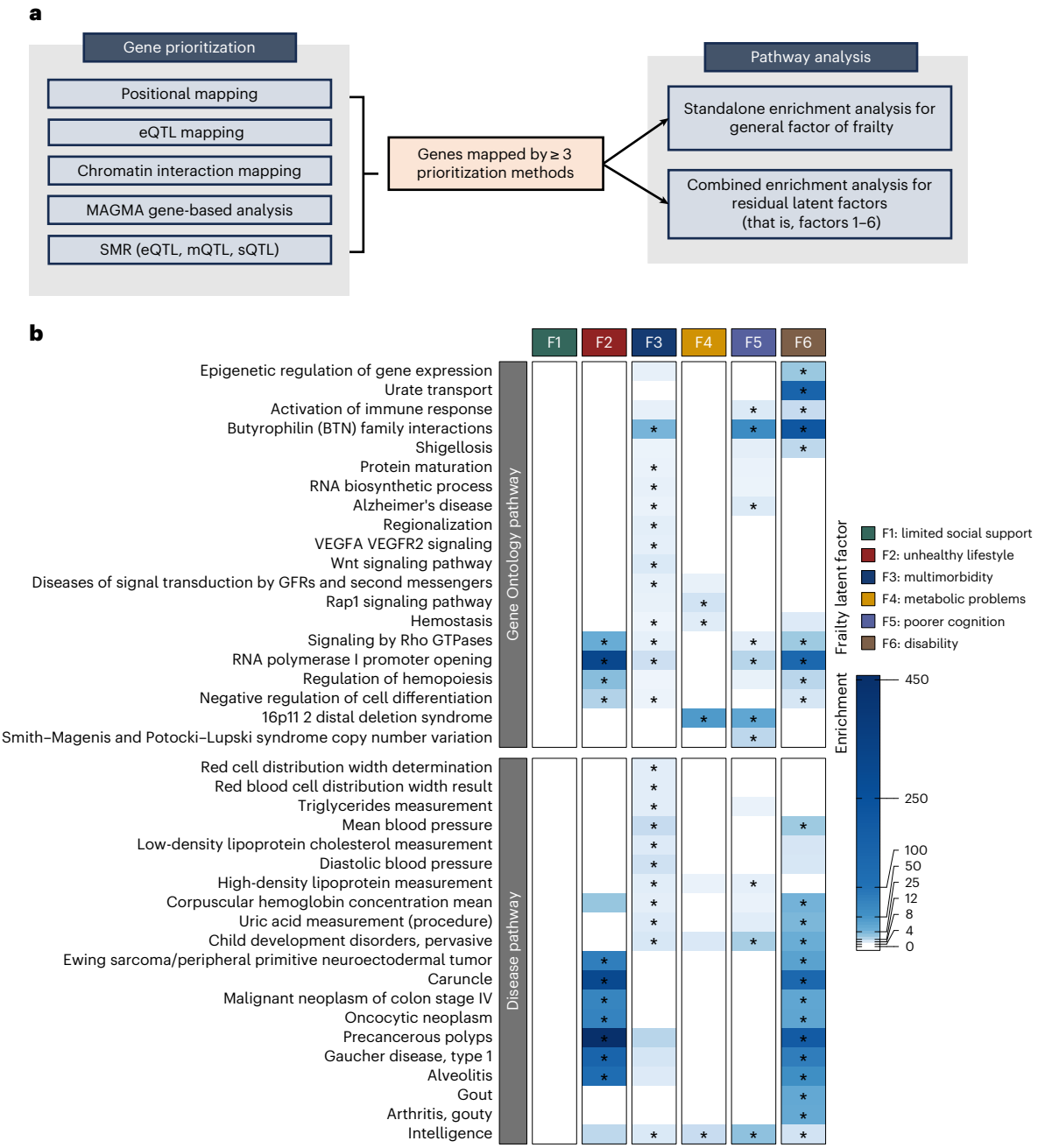

Fig. 5 | Overview of the gene prioritization pipeline and results from the pathway enrichment analysis for the residual frailty factors. a, Overview of the methods used to conduct gene prioritization and subsequent pathway analysis for the latent frailty factor GWAS results. **b**, Heatmaps of the results for the combined pathway enrichment analysis of the residual frailty factors (that is, factors 1–6). Top: the heatmap shows the results for the top 20 most enriched Gene Ontology pathway clusters. The displayed values represent the enrichment value for the most significant Gene Ontology term in each cluster (as named on the *y* axis). Bottom: the heatmap displays the results for the top 20 most significantly enriched disease pathways from the DisGeNET database. There were no significantly enriched pathways for factor 1 (limited social support) because only four genes (*CTNND1*, *TMX2*, *MED19* and *EGR3*) were mapped to that latent factor. FDR correction was used to account for multiple testing; significant enrichment values are marked with an asterisk (that is, one-sided $q < 0.05$). GFR, growth factor receptor; mQTL, methylation QTL; sQTL, splicing QTL; VEGFA/R2, vascular endothelial growth factor A/receptor 2.

analysis separately for that factor but performed a combined analysis for factors 1–6 to account for the potential overlap in implicated gene pathways owing to the presence of inter-factor correlations between these latent residual factors.

Pathway analysis of the prioritized genes for the general factor identified only two significantly enriched disease pathways for intelligence and scoliosis (Supplementary Tables 38–40). In contrast, we found high levels of significant enrichment (that is, $q < 0.05$) for all residual latent frailty factors, except for factor 1 (Fig. 5 and Supplementary Tables 41–43). The most strongly enriched pathway cluster (lead Gene Ontology term = RNA polymerase I promoter opening) included multiple gene sets linked to known aging-related processes, including telomere function, amyloid fiber formation and oxidative stress, and was significantly enriched across factors 2 (unhealthy lifestyle), 3 (multimorbidity), 5 (poorer cognition) and 6 (disability). Other pervasive cross-factor enrichment implicated immune function, epigenetic regulation and cancer as key pathways involved in frailty pathogenesis. In addition to the shared enrichment

in aging-related pathways observed across the factors, we also found evidence for discriminant validity of frailty factors. For example, only factors 3 (multimorbidity) and 5 (poorer cognition) demonstrated significant enrichment for pathways linked to Alzheimer's disease and general neurodegeneration. Factor 3 (multimorbidity) was also enriched in protein maturation and folding pathways, providing consistent evidence that aspects of frailty related to multimorbidity and cognition may be more highly linked to dementia and neurodegenerative pathways compared to other aspects of frailty. Factor 4 (metabolic problems) genes were enriched in gene sets linked to cell signaling (particularly the Rap1 pathways) and 16p11.2 distal deletion syndrome. This is a rare syndrome that results from the partial deletion of the short arm of chromosome 16, leading to symptoms including intellectual disability, developmental delay and autism spectrum disorder. This syndrome can be caused by unmasked recessive mutations in the *CLN3* gene[23], which was where the most significant risk locus for our frailty GWAS was located (lead SNP rs27741; factor 4 $P = 1.09 \times 10^{-35}$) (Fig. 3). Enrichment analysis of the disease pathways from the DisGeNET database further demonstrated that frailty factors display a distinct underlying biology. Factor 3 (multimorbidity) genes were strongly enriched in pathways linked to red blood cell and lipid biomarkers, whereas factors 2 (unhealthy lifestyle) and 6 (disability) genes were significantly enriched in cancer pathways, and additionally, in gout and arthritis pathways for factor 6.

Polygenic risk scores predict frailty in external cohorts

To validate latent frailty factors as phenotypes that capture frailty-specific variance, we created polygenic risk scores (PRSs) for each latent frailty factor and used regression models to test how well they predicted frailty and frailty-related outcomes in three external older adult cohorts (the Lothian Birth Cohort 1936 (LBC1936) ($n = 1{,}005$; mean age = 69.60), the English Longitudinal Study of Aging (ELSA) ($n = 7{,}181$, mean age = 68.45) and the Prospective Imaging Study of Aging (PISA) ($n = 3{,}265$, mean age = 60.34)) (Methods and Supplementary Note). To measure the cumulative predictive capacity of our frailty model, we also created a PRS phenotype that combined the polygenic signal of all seven frailty factors using multiple regression (herein referred to as multi-PRS). This allowed us to compare the performance of our overarching multivariate model in predicting frailty status relative to PRSs created from existing aggregate frailty GWAS measures (that is, the FI-PRS[20] and FP-PRS[21]). The combined multi-PRS provided the strongest prediction of the FI in PISA and ELSA and was comparable to the FI-PRS in LBC1936 (Fig. 6a and Supplementary Table 44). Furthermore, the individual PRS for each latent factor, except for the PRS for factor 1 (limited social support), were significantly associated with FI status in at least two of the three cohorts, indicating that these construct capture frailty-relevant genetic variance (Fig. 6b and Supplementary Table 44).

To assess the influence of sex and age on the latent frailty factors, we split each of the latent factor PRS phenotypes into quintiles (Methods). None of the cohorts demonstrated significant associations between the PRS quintiles and sex. In contrast, significant associations between increasing age and higher PRS quintiles were observed for the F2-PRS ($F = 2.71$, $P = 2.86 \times 10^{-2}$), F3-PRS ($F = 3.55$, $P = 6.78 \times 10^{-3}$), GF-PRS ($F = 2.88$, $P = 2.14 \times 10^{-2}$) and the multi-PRS ($F = 4.90$, $P = 6.00 \times 10^{-4}$) in ELSA, the F4-PRS ($F = 2.46$, $P = 4.36 \times 10^{-2}$) in PISA and the multi-PRS ($F = 3.29$, $P = 1.09 \times 10^{-2}$) in LBC1936.

We additionally measured the association of the latent frailty PRSs with other frailty-related health outcomes, which helped provide a more detailed picture of how these frailty subgroupings may differentially affect aging processes (Supplementary Table 45 and Supplementary Note). We found that the PRS for factor 5 (poorer cognition) and the multi-PRS significantly predicted lower cognitive ability in LBC1936 ($\beta = -0.68$, s.e. = 0.10, $q = 4.03 \times 10^{-9}$ and $\beta = -0.59$; s.e. = 0.10, $q = 4.63 \times 10^{-7}$), but not cognitive change. The PRS for factor 5 (poorer cognition) was also significantly associated with reduced visuospatial reasoning in PISA ($\beta = -0.11$, s.e. = 0.03, $q = 5.64 \times 10^{-4}$).

We used elastic net regression to jointly model the PRS for the seven frailty factors so that we could rank the order that each contributed to predicting frailty status (Fig. 6c–e and Supplementary Table 46). The general factor of frailty was ranked as the highest contributor to FI prediction in all three tested cohorts. We also used elastic net regression to rank the performance of the full latent frailty model (multi-PRS) against the previously derived aggregate frailty GWAS measures (FI-PRS and FP-PRS). We found that the multi-PRS outperformed the FI-PRS and FP-PRS when predicting FI status in ELSA and PISA (Fig. 6f–h and Supplementary Table 47). Sensitivity analyses that grouped samples according to age demonstrated that the predictive contributions of the latent factor PRS remained consistent in the older age groups (Supplementary Note). Together, these findings validated our model as representing a new genetic measure that captures frailty-relevant pathways, which explained more genetic variance than aggregate GWAS measures used in the field so far.

Discussion

Here we report a genomic factor analysis of frailty. We introduce seven new latent constructs of the shared genetics between 30 frailty deficits, including a general factor of frailty and six additional residual factors representing genetic overlap between distinct subsets of frailty deficits. Qualitatively, the six residual factors represent issues related to limited social support, unhealthy lifestyle, multimorbidity, metabolic problems, poorer cognition and disability. We identified 408 genomic risk loci for these latent constructs that are enriched for pathways related to accelerated aging, including epigenetic modifications and immune regulation. This demonstrates a substantial advance in genomic locus discovery for frailty compared to prior GWAS of aggregate frailty measures, which only identified 14 genomic loci for the FI[20] and 37 genomic loci for the FP[21]. We further validated the latent constructs as being relevant to frailty and related health outcomes at multiple levels of biology and in the prediction of frailty status in external data.

Our findings support previous phenotypic studies that highlight the merit, relative to single aggregate scores, of using data reduction methods to improve our understanding of frailty etiology[12,24,25]. However, by taking a multivariate genomic approach, we were able to integrate theoretical knowledge with biological evidence to better define the underlying pathways of frailty and to differentiate generalized pathogenic pathways from more nuanced pathways that are specific to a subset of deficits, both of which are fundamental to understanding this complex clinical construct. For example, our genetic correlation and pathway analyses implicate immune function and epigenetic modifications as being key drivers of frailty pathogenesis across multiple deficit groupings. This is in line with findings linking frailty and elevated C-reactive protein levels, red blood cell distribution width and white blood cell count[26–29]. Our frailty factors were also significantly genetically correlated with health complications associated with infection, including hospitalization and sepsis. The associations between frailty and common viral infections, such as pneumonia[30], coronavirus disease 2019[31] and urinary tract infections[32] are well documented. Furthermore, our findings consistently demonstrated evidence for widespread epigenetic changes in frailty, supporting previous work suggesting that epigenetic biomarkers, such as epigenetic clocks[33] or epigenetic risk scores[34], could be effective predictors of frailty. At the gene level, our analyses prioritized potential causal genes related to distinct frailty subgroups that may help to refine our understanding of frailty biology, even in scenarios where a gene has widespread effects. For example, the *MEF2C* gene has an important role in cardiovascular, neurological and musculoskeletal development, as well as metabolic regulation[35–37]. However, *MEF2C* only mapped to the poorer cognition latent factor (factor 5) in our study, indicating that its role on cognitive function[38] seems to be the key pathway related to frailty.

https://doi.org/10.1038/s41588-025-02269-0

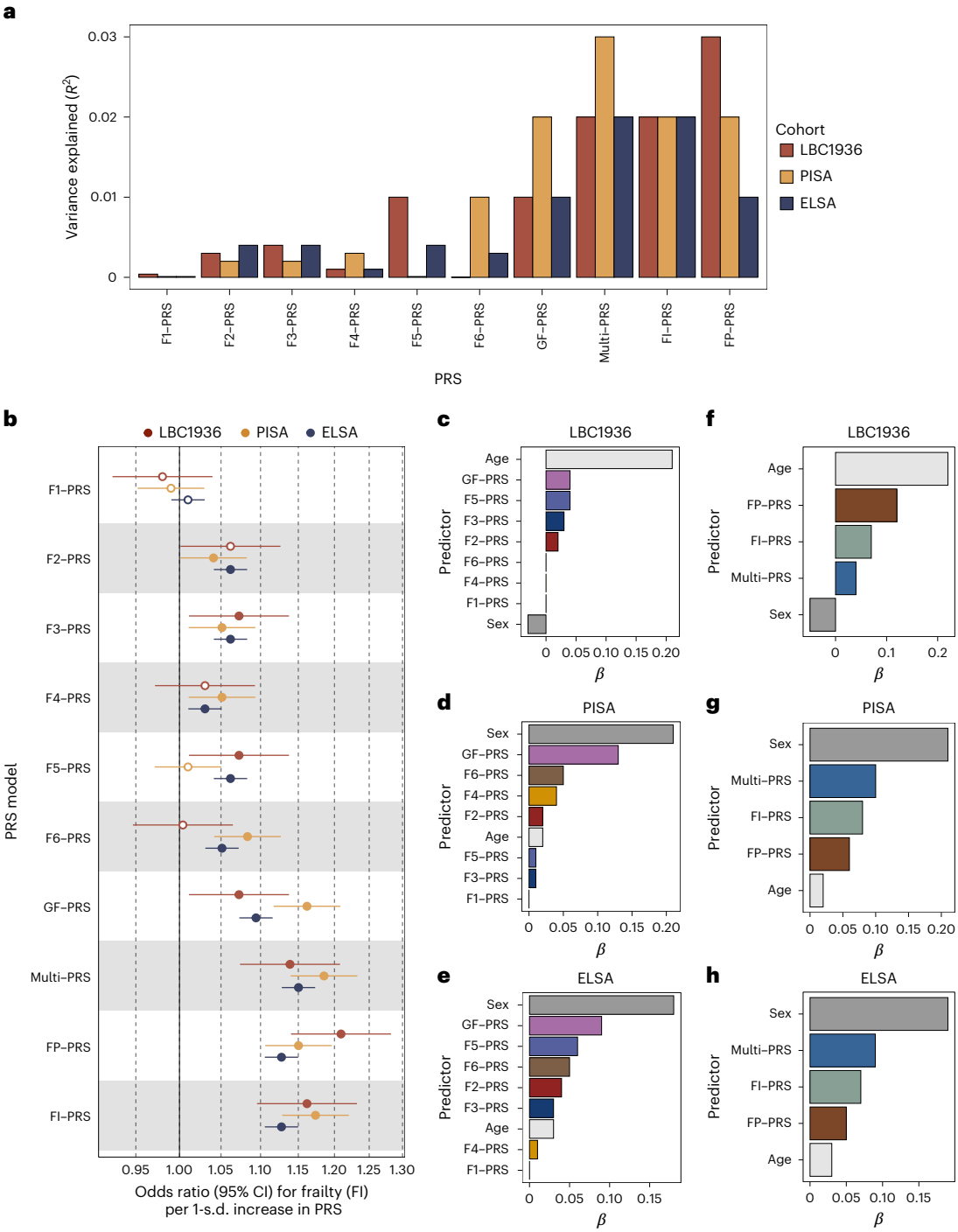

Fig. 6 | Results from the PRS analyses of the latent frailty factors conducted in the LBC1936 (n = 1,005), PISA (n = 3,265) and ELSA (n = 7,181) cohorts. **a**, Bar plot of the variance explained (R^2) by each PRS that we estimated to predict the FI in each external cohort. **b**, Forest plot of the estimated odds ratios for frailty (measured by the FI) per s.d. of the PRS distribution for each latent frailty factor in each external cohort. Data are represented as odds ratios and their corresponding 95% confidence intervals (CIs) as the error bars. These values were calculated using linear regression models. We applied FDR correction to account for multiple testing and significant predictions (that is, two-sided $q < 0.05$) are depicted as filled circles, whereas nonsignificant predictions are depicted as empty circles. **c**–**e**, Bar plots of the elastic net regression analyses ranking the contributions of the seven latent frailty factors in predicting frailty status in LBC1936 (**c**), PISA (**d**) and ELSA (**e**). Each model included all seven latent factor PRS as well as age, sex and ancestral PCs as covariates. **f**–**h**, Bar plots of the elastic net regression analyses that ranked the performance of our multi-PRS (that is, combined latent frailty factor score) when modeled with the aggregate FI-PRS, the aggregate FP-PRS, and age, sex and ancestral PCs included as covariates in LBC1936 (**f**), PISA (**g**) and ELSA (**h**). All analyses represent standardized results.

The seven frailty factors displayed discriminant validity across multiple levels of biological analysis, indicating that existing aggregate measures of frailty are likely to miss clinically relevant distinctions. For example, we found that the poorer cognition factor (factor 5) was the only latent frailty factor that displayed significant genetic overlap with Alzheimer's disease. In addition, our GWAS and gene prioritization findings implicated *SPI1* as a key locus for factor 5, which is a well-replicated Alzheimer's disease risk locus[39–41]. Interestingly, factor 5 had similar factor loadings from lower fluid intelligence and poor self-reported overall health rating, indicating that subjective health

reports, as well as cognitive testing, could be indicative of subsequent heightened Alzheimer's disease risk in individuals who present with these frailty deficits. In fact, subjective cognitive decline has been widely supported as a potential early marker of cognitive impairment[42]. The other loading onto this latent factor was slow walking pace, which is independently associated with heightened dementia risk[43]. In addition, slow gait and subjective cognitive decline are used to measure motoric cognitive risk, a syndrome strongly associated with subsequent dementia[44].

Furthermore, our genetic correlation found that the multimorbidity factor (defined by the number of illnesses and high mean arterial pressure) is a strong driver of frailty over and above the variance captured by a general aggregate measure of all frailty deficits. Prevalence of multimorbidity and associated polypharmacy is a global public health concern, with rates as high as 90% in certain populations[45]. This latent factor produced by far the highest number of genomic risk loci and PRS analyses demonstrated that its predictive power was consistently strong across the external cohorts. Gene prioritization and pathway analysis indicated enrichment in a wide array of aging-related pathways, including *VEGFA* SIGNALING, which was recently identified in a multivariate GWAS of aging[46] and has been shown to be important in longevity[47]. Taken together, our findings suggest that this latent factor includes a broad set of disease-related biological pathways that are associated with the most common diseases found in populations that lead to a heightened risk for developing frailty and accelerated aging. This provides empirical support for the 'geroscience hypothesis', which theorizes that manipulating aging physiology will prevent associated diseases[48].

Our findings should be viewed in light of several limitations. We did not explore the impact of sex differences, which are important in aging as evidenced by significant prevalence differences in frailty across all age groups[49]. Our tissue enrichment analyses alluded to this with significant enrichment identified for the sex-specific reproductive organs. However, sex chromosomes are often excluded from GWAS results[50], and multivariate methods designed for analyzing this type of data are currently lacking. As data and methods become available, future work should examine the influence of genetic variation in the sex chromosomes on the sex-specific prevalence and clinical manifestations of frailty. Furthermore, our analyses were restricted to samples of European genetic ancestry as the methods rely on linkage disequilibrium information that can vary across ancestral populations. Unfortunately, despite advances in collecting genomic data from multiple populations, it was not possible to identify publicly available GWAS data for the frailty deficits to conduct a multi-ancestry analysis, but this should be a major focus in the future to make these results more generalizable globally. Finally, the labels of the six residual latent factors in our model should be interpreted as non-definitive, theoretical approximations of the genetic variance that underpins them. This is an inherent feature of SEM approaches more generally as the shared variance captured by a latent factor is, by design, representative of an unmeasured construct. Therefore, we had to combine our empirical results with theoretical reasoning to determine what shared processes we believed these latent factors are capturing (see the Supplementary Note for justification of the factor names used).

In conclusion, we have introduced a genomic latent model of frailty and demonstrated the added potential of modeling frailty as multiple latent factors, representing both a generalized pathway of frailty and distinct subgroups of deficits that share an additional underlying biology. This can be contrasted with previous studies that have relied solely on aggregate measures of frailty. This more nuanced model offers unique etiological insights into frailty and may aid in refining risk stratification of patients. Our genomic model of frailty may also help to develop new preventive and therapeutic strategies that minimize the broad range of adverse frailty-related health outcomes.

Online content

Any methods, additional references, Nature Portfolio reporting summaries, source data, extended data, supplementary information, acknowledgements, peer review information; details of author contributions and competing interests; and statements of data and code availability are available at https://doi.org/10.1038/s41588-025-02269-0.

References

1. Fogg, C. et al. The dynamics of frailty development and progression in older adults in primary care in England (2006–2017): a retrospective cohort profile. *BMC Geriatr.* **22**, 30 (2022).
2. Kojima, G., Iliffe, S. & Walters, K. Frailty index as a predictor of mortality: a systematic review and meta-analysis. *Age Ageing* **47**, 193–200 (2018).
3. Park, C. M. et al. Frailty and hospitalization-associated disability after pneumonia: a prospective cohort study. *BMC Geriatr.* **21**, 111 (2021).
4. O'Caoimh, R. et al. Prevalence of frailty in 62 countries across the world: a systematic review and meta-analysis of population-level studies. *Age Ageing* **50**, 96–104 (2021).
5. Young, A. C. M., Glaser, K., Spector, T. D. & Steves, C. J. The identification of hereditary and environmental determinants of frailty in a cohort of UK twins. *Twin Res. Hum. Genet.* **19**, 600–609 (2016).
6. Mitnitski, A. B., Mogilner, A. J. & Rockwood, K. Accumulation of deficits as a proxy measure of aging. *Sci. World J.* **1**, 323–336 (2001).
7. Fried, L. P. et al. Frailty in older adults: evidence for a phenotype. *J. Gerontol. A* **56**, M146–M157 (2001).
8. Howlett, S. E., Rutenberg, A. D. & Rockwood, K. The degree of frailty as a translational measure of health in aging. *Nat. Aging* **1**, 651–665 (2021).
9. Ritchie, S. J., Tucker-Drob, E. M., Starr, J. M. & Deary, I. J. Do cognitive and physical functions age in concert from age 70 to 76? Evidence from the Lothian Birth Cohort 1936. *Span. J. Psychol.* **19**, E90 (2016).
10. Zhang, X. et al. Association between physical, psychological and social frailty and health-related quality of life among older people. *Eur. J. Public Health* **29**, 936–942 (2019).
11. Lachmann, R. et al. The accumulation of deficits approach to describe frailty. *PLoS ONE* **14**, e0223449 (2019).
12. Pridham, G., Rockwood, K. & Rutenberg, A. Efficient representations of binarized health deficit data: the frailty index and beyond. *Geroscience* **45**, 1687–1711 (2023).
13. Grotzinger, A. D. et al. Genomic structural equation modelling provides insights into the multivariate genetic architecture of complex traits. *Nat. Hum. Behav.* **3**, 513–525 (2019).
14. López-Otín, C., Blasco, M. A., Partridge, L., Serrano, M. & Kroemer, G. Hallmarks of aging: an expanding universe. *Cell* **186**, 243–278 (2023).
15. Wray, N. R. et al. Genome-wide association analyses identify 44 risk variants and refine the genetic architecture of major depression. *Nat. Genet.* **50**, 668–681 (2018).
16. Trpchevska, N. et al. Genome-wide association meta-analysis identifies 48 risk variants and highlights the role of the stria vascularis in hearing loss. *Am. J. Hum. Genet.* **109**, 1077–1091 (2022).
17. Watanabe, K. et al. Genome-wide meta-analysis of insomnia prioritizes genes associated with metabolic and psychiatric pathways. *Nat. Genet.* **54**, 1125–1132 (2022).
18. Liu, M. et al. Association studies of up to 1.2 million individuals yield new insights into the genetic etiology of tobacco and alcohol use. *Nat. Genet.* **51**, 237–244 (2019).
19. Jones, G. et al. Genome-wide meta-analysis of muscle weakness identifies 15 susceptibility loci in older men and women. *Nat. Commun.* **12**, 654 (2021).

20. Atkins, J. L. et al. A genome-wide association study of the frailty index highlights brain pathways in ageing. *Aging Cell* **20**, e13459 (2021).
21. Ye, Y. et al. A genome-wide association study of frailty identifies significant genetic correlation with neuropsychiatric, cardiovascular, and inflammation pathways. *Geroscience* **45**, 2511–2523 (2023).
22. Zhou, Y. et al. Metascape provides a biologist-oriented resource for the analysis of systems-level datasets. *Nat. Commun.* **10**, 1523 (2019).
23. Pebrel-Richard, C. et al. An unusual clinical severity of 16p11.2 deletion syndrome caused by unmasked recessive mutation of *CLN3*. *Eur. J. Hum. Genet.* **22**, 369–373 (2014).
24. Liotta, G. et al. Exploratory factor analysis (EFA) of the Short Functional Geriatric Evaluation (SFGE) to assess the multidimensionality of frailty in community-dwelling older adults. *Int. J. Environ. Res. Public Health* **20**, 4129 (2023).
25. Johnson, L. et al. Frailty or frailties: exploring frailty index subdimensions in the English Longitudinal Study of Ageing. *J. Epidemiol. Community Health* **78**, 609–615 (2024).
26. Soysal, P. et al. Inflammation and frailty in the elderly: a systematic review and meta-analysis. *Ageing Res. Rev.* **31**, 1–8 (2016).
27. Pothier, K., Gana, W., Bailly, N. & Fougère, B. Associations between frailty and inflammation, physical, and psycho-social health in older adults: a systematic review. *Front. Psychol.* **13**, 805501 (2022).
28. Cheng, Z. et al. C-reactive protein and white blood cell are associated with frailty progression: a longitudinal study. *Immun. Ageing* **19**, 29 (2022).
29. Li, C.-M., Chao, C.-T., Chen, S.-I., Han, D.-S. & Huang, K.-C. Elevated red cell distribution width is independently associated with a higher frailty risk among 2,932 community-dwelling older adults. *Front. Med.* **7**, 470 (2020).
30. Iwai-Saito, K., Shobugawa, Y., Aida, J. & Kondo, K. Frailty is associated with susceptibility and severity of pneumonia in older adults (a JAGES multilevel cross-sectional study). *Sci. Rep.* **11**, 7966 (2021).
31. Sablerolles, R. S. G. et al. Association between Clinical Frailty Scale score and hospital mortality in adult patients with COVID-19 (COMET): an international, multicentre, retrospective, observational cohort study. *Lancet Healthy Longev.* **2**, e163–e170 (2021).
32. Chao, C.-T., Lee, S.-Y., Wang, J., Chien, K.-L. & Huang, J.-W. Frailty increases the risk for developing urinary tract infection among 79,887 patients with diabetic mellitus and chronic kidney disease. *BMC Geriatr.* **21**, 349 (2021).
33. Verschoor, C. P. et al. Epigenetic age is associated with baseline and 3-year change in frailty in the Canadian Longitudinal Study on Aging. *Clin. Epigenetics* **13**, 163 (2021).
34. Li, X. et al. Derivation and validation of an epigenetic frailty risk score in population-based cohorts of older adults. *Nat. Commun.* **13**, 5269 (2022).
35. Materna, S. C., Sinha, T., Barnes, R. M., Lammerts van Bueren, K. & Black, B. L. Cardiovascular development and survival require *Mef2c* function in the myocardial but not the endothelial lineage. *Dev. Biol.* **445**, 170–177 (2019).
36. Anderson, C. M. et al. Myocyte enhancer factor 2C function in skeletal muscle is required for normal growth and glucose metabolism in mice. *Skelet. Muscle* **5**, 7 (2015).
37. Cooley Coleman, J. A. et al. Comprehensive investigation of the phenotype of *MEF2C*-related disorders in human patients: a systematic review. *Am. J. Med. Genet. A* **185**, 3884–3894 (2021).
38. Barker, S. J. et al. MEF2 is a key regulator of cognitive potential and confers resilience to neurodegeneration. *Sci. Transl. Med.* **13**, eabd7695 (2021).
39. Bellenguez, C. et al. New insights into the genetic etiology of Alzheimer's disease and related dementias. *Nat. Genet.* **54**, 412–436 (2022).
40. Wightman, D. P. et al. A genome-wide association study with 1,126,563 individuals identifies new risk loci for Alzheimer's disease. *Nat. Genet.* **53**, 1276–1282 (2021).
41. Schwartzentruber, J. et al. Genome-wide meta-analysis, fine-mapping and integrative prioritization implicate new Alzheimer's disease risk genes. *Nat. Genet.* **53**, 392–402 (2021).
42. Parfenov, V. A., Zakharov, V. V., Kabaeva, A. R. & Vakhnina, N. V. Subjective cognitive decline as a predictor of future cognitive decline: a systematic review. *Dement. Neuropsychol.* **14**, 248–257 (2020).
43. Gao, P.-Y. et al. Physical frailty, genetic predisposition, and incident dementia: a large prospective cohort study. *Transl. Psychiatry* **14**, 212 (2024).
44. Mullin, D. S., Gadd, D., Russ, T. C., Luciano, M. & Muniz-Terrera, G. Motoric cognitive risk syndrome trajectories and incident dementia over 10 years. *Cereb. Circ. Cogn. Behav.* **5**, 100178 (2023).
45. Nicholson, K. et al. Prevalence of multimorbidity and polypharmacy among adults and older adults: a systematic review. *Lancet Healthy Longev.* **5**, e287–e296 (2024).
46. Rosoff, D. B. et al. Multivariate genome-wide analysis of aging-related traits identifies novel loci and new drug targets for healthy aging. *Nat. Aging* **3**, 1020–1035 (2023).
47. Grunewald, M. et al. Counteracting age-related VEGF signaling insufficiency promotes healthy aging and extends life span. *Science* **373**, eabc8479 (2021).
48. Sierra, F. & Kohanski, R. Geroscience and the trans-NIH Geroscience Interest Group, GSIG. *Geroscience* **39**, 1–5 (2017).
49. Gordon, E. H. et al. Sex differences in frailty: a systematic review and meta-analysis. *Exp. Gerontol.* **89**, 30–40 (2017).
50. Sun, L., Wang, Z., Lu, T., Manolio, T. A. & Paterson, A. D. eXclusionarY: 10 years later, where are the sex chromosomes in GWASs? *Am. J. Hum. Genet.* **110**, 903–912 (2023).

[1]Institute for Behavioral Genetics, University of Colorado Boulder, Boulder, CO, USA. [2]Centre for Preventive Neurology, Wolfson Institute of Population Health, Queen Mary University of London, London, UK. [3]Lothian Birth Cohorts, University of Edinburgh, Edinburgh, UK. [4]Department of Psychology, School of Philosophy, Psychology and Language Sciences, University of Edinburgh, Edinburgh, UK. [5]Advanced Care Research Centre School of Engineering, College of Science and Engineering, University of Edinburgh, Edinburgh, UK. [6]Brain and Mental Health Program, QIMR Berghofer Medical Research Institute, Brisbane, Queensland, Australia. [7]Alzheimer Scotland Dementia Research Centre, University of Edinburgh, Edinburgh, UK. [8]Department of Psychology and Neuroscience, University of Colorado Boulder, Boulder, CO, USA. [9]Centre for Clinical Brain Sciences,

Division of Psychiatry, University of Edinburgh, Edinburgh, UK. [10]Nova Scotia Health, Halifax, Nova Scotia, Canada. [11]Division of Geriatric Medicine, Dalhousie University, Halifax, Nova Scotia, Canada. [12]Department of Pharmacology, Dalhousie University, Halifax, Nova Scotia, Canada. [13]Department of Physics and Atmospheric Science, Dalhousie University, Halifax, Nova Scotia, Canada. [14]School of Biomedical Sciences, Faculty of Medicine, The University of Queensland, Brisbane, Queensland, Australia. [15]School of Biomedical Sciences, Faculty of Health, Queensland University of Technology, Brisbane, Queensland, Australia. [16]University of Exeter Medical School, University of Exeter, Exeter, UK. [17]Alan Turing Institute, London, UK. ✉e-mail: isabelle.foote@colorado.edu

Methods

Ethics

Ethical approval was not required for most of the analyses in this study because they used publicly available summary data only. However, for the PRS analyses that required access to individual-level data, we received ethical approval from the relevant study boards for each external cohort (Supplementary Note).

Phenotype selection

Phenotypes were selected based on the deficits described by the FI[51]. We specifically included traits that reflected systemic pathways and health behaviors (for example, number of diagnosed illnesses) as opposed to specific clinical diagnoses (for example, type 2 diabetes) to model genetic variance for general aspects of frailty rather than disease-specific pathways. Traits were included if they had GWAS summary statistics that were publicly available in a sample of 10,000 or more individuals of European ancestry. Analyses were restricted to European ancestry because the methods used to estimate genetic overlap rely on ancestry-specific patterns of linkage disequilibrium and GWAS of sufficient sample size in other ancestry groups are not yet available across all the frailty traits. We prioritized the use of GWAS data from consortium-based studies because these tend to pool the largest sample sizes and have more rigorous phenotypic definitions[15–19,52–57]. When consortia data were not available, we used GWAS summary statistics downloaded from the Pan-UK Biobank (https://pan.ukbb.broadinstitute.org). Supplementary Table 1 summarizes the 52 traits included in our initial analysis. The effect estimates for each trait were formatted in a direction that reflected the 'risk-inducing' phenotype for frailty.

We initially conducted multivariable linkage disequilibrium score regression (LDSC) using the default parameters in the GenomicSEM R package to estimate the SNP-based heritability (h^2_{SNP}) of each deficit phenotype and the bivariate genetic correlations (r_g) between each pair of frailty deficits[13]. We used these results to guide the selection of frailty deficits that could be reliably included in a multivariate latent model (Supplementary Note). This resulted in a final list of 30 traits that were brought forward for all subsequent analyses (Supplementary Table 1). An FI constructed with 30 or more deficits has been shown to sufficiently capture frailty[8].

Genomic factor analysis

Exploratory factor analysis. As the latent pattern of the shared genetic architecture between frailty deficits had not been assessed previously, we initially ran an exploratory factor analysis (EFA) using the stats R package to identify a plausible latent structure that describes the genetic overlap across the included frailty deficits. To avoid model overfitting, we used the genetic covariance matrix estimated in odd autosomes as the input to the EFA and the genetic covariance matrix estimated in even autosomes as the input for the subsequent CFA. We used the Kaiser rule[58] and the number of optimal coordinates test[59] to determine the number of factors to extract in the EFA; both suggested that seven factors were appropriate. We additionally extracted a six-factor model (Supplementary Table 48) as there was a high number of cross-loadings in the seven-factor specification, indicating that a more parsimonious structure may be appropriate, and the fifth factor in the seven-factor model only captured genetic variance related to mean arterial pressure (Supplementary Table 49). We applied promax factor rotation, which allows for inter-factor correlations.

Confirmatory factor analysis. We then conducted a CFA using the diagonally weighted least squares method and the genetic covariance matrix from the even autosomes as input. The CFA model was guided using the EFA results, where a frailty deficit was specified to load on a factor when standardized loadings were 0.30 or greater. The six-factor (CFI = 0.92; SRMR = 0.07) and seven-factor model specification (CFI = 0.89; SRMR = 0.07) both provided a good fit to the even autosome data (Supplementary Table 50). The six-factor model was selected over the seven-factor model because it (1) provided improved fit to the data while offering a more parsimonious representation of the data; (2) produced more theoretically interpretable factors of latent genetic architecture between distinct groups of multiple frailty deficits; and (3) continued to provide good fit to the data in all autosomes (CFI = 0.92; SRMR = 0.06) (Supplementary Table 51).

Bifactor model. While the six-factor model produced theoretically meaningful latent factors, the first latent factor displayed strong factor loadings for 16 of the 30 frailty deficits and the model included pervasive cross-loadings of frailty deficits on multiple factors. This indicated that a bifactor model was an appropriate way to capture the general frailty pathways across all included deficits, as well as the genetic variance specific to distinct subsets of deficits.

Therefore, we estimated the fit of a bifactor model that included loadings for all 30 frailty deficits onto a general factor of frailty (general factor), in addition to the loadings on the six latent factors from the CFA model (factors 1–6). A key benefit to this approach is that the general factor is orthogonal (that is, uncorrelated) to the additional residual group factors, which enabled us to interpret the general factor as general genetic pathways of frailty that are distinct from the more focused subsets of genetic variance that underlie potential subgroups within the frailty spectrum. A bifactor model thereby provided a more direct test of our hypothesis that aggregate scores of frailty (for example, the FI and FP) miss unique risk pathways that are only shared between smaller subsets of frailty deficits.

Owing to the inclusion of the general factor, some of the original factor loadings for the six CFA factors became nonsignificant. We iteratively removed any loadings from factors 1–6 that were less than 0.30 to ensure that we only retained stable loadings in the final model specification. In cases where an indicator displayed loadings above our cutoff for multiple residual factors, we retained these cross-loadings because a previous simulation study found that omitting substantial cross-loadings from a bifactor model based on a prior CFA model can upwardly bias the general factor loadings and downwardly bias residual group factor loadings, which cannot be picked up using standard model fit measures[60].

We allowed the residual group factors (factors 1–6) to be correlated (but orthogonal to the general factor). This form of bifactor model is known as a bifactor (S-1) model and is sufficiently identified if a subset of the indicators only load onto the bifactor (in our case 50% of the frailty deficits solely loaded onto the bifactor)[61]. To ensure the model was locally identified, factor loadings were constrained to be equal when there were only two indicators that loaded onto a factor (that is, for factors 1 and 3). The final bifactor (S-1) model (Fig. 1 and Supplementary Table 3) continued to provide good fit to the data (CFI = 0.93; SRMR = 0.07) and was brought forward for all subsequent analyses.

Genetic correlations with related health traits

Frailty is known to increase the risk of many adverse health outcomes, but it is unclear whether this is because of shared genetics between the more general frailty pathways or whether some outcomes are only associated with certain deficits in the frailty state. Furthermore, as this represented the first time that frailty has been measured in this latent framework, we wanted to validate that our factors reflected frailty. Therefore, we used genomic SEM to calculate the genetic correlations between 52 aging-related health outcomes and existing frailty phenotypes and each of the latent frailty factors (Supplementary Tables 4 and 5)[20,21,62–81]. We used the same quality control procedures on the GWAS summary statistics for these outcomes as described for the main frailty deficits (Supplementary Note) and used an FDR-corrected $q < 0.05$ threshold to correct for multiple testing. However, in the case

of pneumonia, there were no prior available GWAS summary statistics with an SNP-based heritability estimate high enough to be included in the LDSC. Therefore, we conducted a fixed-effect meta-analysis using the METAL software, which included GWAS summary statistics data from the Pan-UK Biobank (https://pan.ukbb.broadinstitute.org) (n_{cases} = 14,054 and $n_{controls}$ = 405,999) and FinnGen release 10 (https://r10.finngen.fi/) (n_{cases} = 63,377 and $n_{controls}$ = 348,804). This resulted in a total GWAS sample of 832,234 individuals (n_{cases} = 77,431 and $n_{controls}$ = 754,803), which produced a reasonable SNP-based heritability for LDSC (Supplementary Table 4; *z*-statistic = 4.1).

Multivariate GWAS of latent frailty factors

GWAS estimation. We performed a multivariate GWAS within the GenomicSEM R package that estimated the individual SNP associations with each of the latent factors in our bifactor (S-1) model. After data standardization (Supplementary Note), 5,849,452 SNPs were included in our multivariate GWAS. We fixed the measurement model (that is, the genome-wide factor loadings and factor correlations) for all SNPs. This improved computational tractability and model interpretability as the SNP-specific estimates were scaled according to the same measurement model across all SNPs (as opposed to the entire model being reestimated for each SNP). We removed any SNPs that required a high level of smoothing (that is, *z*-statistic change before and after smoothing greater than 1.96) or that produced lavaan warnings for negative observed variable or latent variable variances or nonpositive definite covariance matrices (293 SNPs removed in total).

Q_{SNP} heterogeneity index. As described previously, not all the genetic signal captured in the latent factor GWAS results represents genuinely shared genetic variance. For example, a strong signal from a single indicator (for example, the *FTO* locus for body fat percentage) can lead to false positives if not properly accounted for[13]. Likewise, some of the nonsignificant genetic signal in the multivariate GWAS results may represent areas of the genome that have highly heterogenous magnitudes and directions of effect on the different univariate indicators[13]. For this reason, it is necessary to calculate the Q_{SNP} heterogeneity statistics for each SNP, which reflects a χ^2-distributed statistic that is higher for SNPs whose effects deviate strongly from the patterning of effects implied by the factor model.

As part of the current project, we introduced and validated a more computationally efficient way of calculating Q_{SNP} using a closed-form estimation method. While the prior model comparison formulation of Q_{SNP} required estimating a series of follow-up models to calculate the heterogeneity statistic[13], our new formulation was automatically calculated for each factor predicted by an SNP in the model. This change thereby greatly reduced the runtime of our analysis. The new closed-form Q_{SNP} equation starts by calculating the residual covariance matrix for the subset of the matrix that reflects the SNP-phenotype covariances for the phenotypes that load on a given factor (R_{SNP}) as:

$$R_{SNP} = S_{SNP} - \sum \theta_{SNP} \quad (1)$$

where S_{SNP} is the vector of SNP-phenotype covariances and $\sum \theta_{SNP}$ reflects the model-implied SNP-phenotype covariances. These model-implied estimates reflect the product of the estimated SNP effect on a given factor and the factor loadings for each trait. The precision of those SNP-phenotype estimates is indexed by taking the eigen decomposition of the portion of the sampling covariance matrix (V) that indexes those SNP-phenotype effects (V_{SNP}):

$$V_{SNP} = (P_1 P_0)\begin{pmatrix} E & 0 \\ 0 & 0 \end{pmatrix}\begin{pmatrix} P_1' \\ P_0' \end{pmatrix} \quad (2)$$

where P_1 is the matrix of PCs (eigenvectors) of V_{SNP}, P_0 is the null space of V_{SNP} and E is a diagonal matrix of the nonzero eigenvalues of V_{SNP}. These eigenvalues and eigenvectors can then be used to weight the residual covariance matrix of the SNP-phenotype estimates to obtain a χ^2-distributed test statistic given as:

$$Q_{SNP}\,(\text{d.f.}) \sim R_{SNP}{}' P_1 E^{-1} P_1{}' R_{SNP} \quad (3)$$

where d.f. reflects the degrees of freedom, which will be one less than the number of indicators for the factor. This equation is iteratively applied for each factor that is predicted by an SNP, such that a separate R_{SNP}, V_{SNP} *and* factor-specific Q_{SNP} are produced.

Via simulation, we demonstrated that this new closed-form approach continues to produce a χ^2-distributed statistic that is statistically equivalent to the previously described model comparison formulation of Q_{SNP}. We used the simulateData function in the lavaan R package to simulate data for three different factor models each with 50,000 observations for 1,000 SNPs. We tested a 2-factor model with 3 indicators on each factor (2 d.f.), a 2-factor model with 4 indicators on each factor (3 d.f.) and a 2-factor model with 6 indicators on each factor (5 d.f.). We confirmed across all three examples that the closed-form method remained χ^2-distributed and that they did not differ significantly from the estimates calculated using the previous model comparison method in terms of the mean Q_{SNP} (Supplementary Note). In addition, the closed-form method consistently demonstrated a well-calibrated type 1 error rate ($P < 0.05$) (Supplementary Note).

For our empirical frailty application, we pruned out the Q_{SNP} significant signal from our GWAS summary statistics for each latent frailty factor to ensure that we only measured shared genetic variance operating via each latent factor in our subsequent post-GWAS analyses. We did this by removing SNPs that had a Bonferroni-corrected Q_{SNP} $P < 7.14 \times 10^{-9}$ (that is, $5 \times 10^{-8}/7$), and any SNPs that were within a 1-Mb window upstream or downstream of this location to ensure that variants that were in linkage disequilibrium with these heterogenous regions were removed.

Once the Q_{SNP} signal had been pruned from the latent factor summary statistics, we used the method developed by Mallard et al.[82] to calculate the expected sample size ($\hat{N}$) of each latent factor. This value quantifies the amount of error-free genetic variance being captured by each latent factor, so it also acts as an indicator of how well powered each latent factor is in the model.

Identification of genomic risk loci for latent frailty factors. We used FUMA v.1.5.2 to identify genomic risk loci for each latent factor in our model[83]. We used a Bonferroni-corrected genome-wide significance threshold of $P < 7.14 \times 10^{-9}$ (that is, $5 \times 10^{-8}/7$ factors) to identify significant SNPs in our pruned GWAS summary statistics for each latent factor (that is, Q_{SNP}-significant variants were removed). A genomic risk locus was defined as the region around a genome-wide significant SNP that included all SNPs that were in linkage disequilibrium ($r^2 \geq 0.6$) with that variant based on the linkage disequilibrium patterns in the 1000 Genomes Project Phase 3 European ancestry reference genome[83]. If there were additional independently significant SNPs in linkage disequilibrium with the lead SNP ($r^2 \geq 0.1$) or if loci were located within 250 kb of one another, these were merged into a single locus[83].

Stratified genomic SEM

As frailty has been consistently linked to increased risk of poorer brain health and dementia, which represents a key burden on health services in aging populations[8], we explored whether there was evidence for brain-relevant functional enrichment in the genetic variance captured by our latent frailty factors. We applied stratified genomic SEM[84] to test whether there was evidence for enrichment in functional annotations (groups of genetic variants combined due to having a shared biological characteristic) that are known to influence tissue-specific gene expression in different brain regions, histone modifications, neuronal cell types or the interaction between these neuronal cell types

and protein-truncating variant-intolerant genes. We used previously constructed functional annotations based on data from the 1000 Genomes Project Phase 3 Baseline LD v.2.2 (ref. 85), Genotype-Tissue Expression (GTEx)[86], DEPICT[87], Roadmap Epigenetics Project[88] and the Genome Aggregation Database[89], which consisted of a total of 172 functional annotations. This included five randomly selected non-brain control regions for the gene expression and histone modifications[90].

We performed multivariable stratified LDSC to estimate the zero-order genetic covariance matrices and the corresponding sampling covariance matrices that were partitioned across the genomic regions of each functional annotation using the s_ldsc function in the GenomicSEM R package[84,85]. We subsequently used these matrices as the input data to the enrich function to calculate an enrichment ratio for the genetic variance captured in each latent factor in our bifactor model for each functional annotation[91]. We removed 26 functional annotations from our analyses because of high degrees of smoothing (defined as a z-score difference greater than 1.96 before and after smoothing), as this indicates low power to detect meaningful enrichment[90]. This resulted in 146 functional annotations being retained in our analyses. We used a $q < 0.05$ threshold to account for multiple testing.

Gene mapping and pathway analysis

Gene mapping. To explore the biological implications of the genomic risk loci underlying each latent frailty factor, we applied five complementary methods to map each locus to potentially causal genes, that is, positional mapping, eQTL mapping, chromatin interaction mapping, MAGMA and multi-SNP SMR (SMR-multi). We used the SNP2GENE function in FUMA (v.1.5.2)[83] to functionally annotate candidate SNPs and map potentially causal genes to each locus based on positional, eQTL and chromatin interaction information (Supplementary Note).

We used MAGMA (v.1.08)[92] to conduct a gene-based analysis that identified genes that were significantly associated with each latent factor. Any measured SNPs that were located in one of the protein-coding genes in the Ensembl database (excluding the major histocompatibility complex region) were analyzed. We used the 1000 Genomes Project Phase 3 European dataset as our linkage disequilibrium reference panel and applied a Bonferroni correction for the number of genes tested in each latent factor GWAS[83]. Using gene expression data from GTEx v.8 for 54 body tissues[93], we also used MAGMA to perform a gene property analysis to ascertain whether the genes significantly associated with the latent factor in the gene-based test were more likely to produce gene expression changes in particular body tissues[94].

Finally, we applied SMR-multi to prioritize genes for each latent frailty factor by identifying SNP-outcome (that is, variant-frailty) associations that demonstrated strong evidence for being driven by pleiotropic effects on gene expression (eQTLs), splicing ratios (sQTLs) or methylation status (mQTLs)[95,96]. Mendelian randomization is a well-established method used to measure the causal influence of an exposure on an outcome using genetic variants as an instrumental variable. For our application of SMR, exposure reflected different measures of gene function (expression, splicing or methylation) and the outcome reflected the different latent frailty deficits identified in genomic SEM (Supplementary Note).

Gene prioritization and pathway analysis. To better understand the underlying biological pathways of each latent frailty factor, we conducted pathway analysis using the genes that had been prioritized by the aforementioned gene mapping analyses as input. However, as not all genes that are mapped to risk loci represent truly causal genes, we triangulated our results to only include genes that presented sustained evidence for being a potential causal candidate for each latent factor. We defined this as any gene that was mapped by three or more of our gene mapping methods (that is, positional mapping, eQTL mapping, chromatin interaction mapping, MAGMA or SMR-multi). We used METASCAPE[22] to perform a pathway enrichment analysis to identify gene sets that were significantly overrepresented in the prioritized genes for each latent factor (Supplementary Note).

Polygenic risk scores

Polygenic risk score construction. To externally validate our frailty latent factors, we constructed PRS of each latent frailty factor and tested whether they predicted frailty and related health outcomes in three external cohort datasets, including LBC1936, ELSA and PISA (see Supplementary Note for the sample descriptions). We used the GWAS summary statistics of the shared genetic signal for each of the latent frailty factors (that is, the summary statistics that had removed a significantly heterogeneous signal), as well as publicly available GWAS summary statistics from previously published studies of aggregate measures for the FI[20] and FP[21] to construct a separate PRS for each of these predictor phenotypes. This enabled us to compare the prediction of the latent frailty factors with routinely used aggregate frailty measures. We performed routine quality control on each of the datasets, including aligning the effect and non-effect alleles to ensure that the direction of effect was concordant across analyses. We removed SNPs with a minor allele frequency of less than 0.01, as well as duplicate and ambiguous SNPs.

After quality control, PRS were calculated for the individuals in each of the three cohorts using SBayesR. We followed default procedures described in detail by the original method developers[97]. Briefly, SBayesR is a Bayesian-based method that estimates joint SNP effects across the genome using multiple linear regression while assuming a finite mixture of normally distributed priors[97].

Prediction of frailty and related phenotypes in the external cohorts. We subsequently performed a series of analyses to explore how well the latent frailty factors predicted routinely measured frailty phenotypes and related traits in external data. First, we used linear regression models to assess how well each individual frailty latent factor PRS predicted the FI in LBC1936 (based on 30 deficits), ELSA (based on 62 deficits) and PISA (based on 69 deficits), and logistic regression models to measure how well they each predicted the FP in LBC1936 (Supplementary Note and Supplementary Tables 52–54). As the latent frailty factors each represented distinct genetic variance that can contribute to frailty, we also used multiple regression to calculate a PRS of the combined scores for all seven latent factors (that is, multi-PRS). Finally, to enable us to compare the performance of the latent factor PRS with previously published frailty GWAS aggregate measures, we also tested how well the FI GWAS PRS (FI-PRS) and the FP GWAS PRS (FP-PRS) predicted the same frailty outcomes in each dataset. All models included age, sex and ancestry PCs (for ELSA and PISA, we used ten PCs and for LBC1936 we used four PCs) as covariates. These models allowed us to calculate the amount of incremental phenotypic variance explained (R^2) by each PRS, which was calculated by subtracting the covariate-only model R^2 from the R^2 of the full PRS and covariate model[98].

To facilitate subgroup analyses examining the effects of sex and age, we categorized each standardized latent factor PRS variable into quintiles. Quintiles were created by dividing the distribution of each PRS into five equal groups based on quantiles (20th, 40th, 60th, 80th and 100th percentiles) using the cut function in R. This ensured that each quintile represented approximately 20% of the sample, with quintile 1 containing the lowest PRS values and quintile 5 containing the highest PRS values. We used χ^2 tests to assess the association between the PRS quintiles and sex, and ANOVA tests to assess whether mean age differed across PRS quintiles.

To assess the association of the latent factor PRS with frailty-related health outcomes, we also conducted regression analyses to test the association of each frailty PRS with cognitive ability (LBC1936), cognitive change (LBC1936), dementia (LBC1936), motoric cognitive risk (LBC1936), mortality (LBC1936), stroke (LBC1936 and PISA), cognition and memory problems (PISA) (Supplementary Note).

Elastic net regression to rank performance of frailty PRS. Finally, as conventional linear regression models can be upwardly biased because of model overfitting, we performed elastic net regularized regression models in all three cohorts to rank the polygenic contributions to frailty while minimizing bias from model overfitting and multicollinearity between predictors[99]. This method allows highly genetically correlated variables to be grouped; the final coefficients returned in the model allow the predictors to be ranked according to their contribution of prediction to the outcome[99]. We used elastic net regression because it combines the strengths of other commonly used prediction methods. For example, ridge regression shrinks coefficients but does not perform feature selection, whereas least absolute shrinkage and selection operator regression performs feature selection but may miss important predictors when variables are correlated. In contrast, elastic net regression performs both shrinkage and feature selection to identify the most important predictors, while also managing multicollinearity[100]. Previous PRS studies demonstrated the usefulness of using elastic net regression modeling when identifying relevant predictors[101–103].

We ran an initial elastic net model predicting the FI in each cohort using the seven individual latent frailty factor PRSs and covariates (age, sex and ancestry PCs) as predictors to rank the latent factors in order of their strength in predicting frailty. We then performed elastic net regression that included the multi-PRS, FI-PRS and FP-PRS and covariates (age, sex and ancestry PCs) to rank the prediction of the different genetic measures of frailty (that is, multiple latent factors versus aggregate measures for the FI and FP).

Reporting summary

Further information on research design is available in the Nature Portfolio Reporting Summary linked to this article.

Data availability

The latent frailty factor and pneumonia GWAS summary statistics created in this study are available at the GWAS Catalog (www.ebi.ac.uk/gwas/; accession nos. GCST90624046–GCST90624053). The frailty PRS created in this study are available at the PGS Catalog (www.pgscatalog.org; accession nos. PGS005221–PGS005229). Individual-level data used for our PRS analyses can be accessed upon reasonable request from the relevant cohorts: LBC1936, PISA and ELSA. The univariate GWAS summary statistics used for our frailty model and the external health outcomes are available via the citations outlined in Supplementary Tables 1 and 4, respectively. The linkage disequilibrium scores and weights, HapMap3 SNPs and 1000 Genomes Project reference file for genomic SEM are available to download at https://utexas.app.box.com/s/vkd36n197m8klbaio3yzoxsee6sxo11v; the functional annotations for conducting the stratified genomic SEM are available via GitHub at https://github.com/genomicsem/genomicsem/wiki/6.-stratified-genomic-sem. The datasets used for positional, eQTL and chromatin interaction mapping and the MAGMA analyses are available at the online platform FUMA (https://fuma.ctglab.nl/); the preprocessed eQTL, sQTL and mQTL data for conducting SMR are available for download at https://yanglab.westlake.edu.cn/software/smr/#DataResource. The databases used for the pathway analysis are available via the online platform METASCAPE at https://metascape.org/gp/index.html#/main/step1.

Code availability

The code was developed using publicly available software available via the following links: R v.4.4.2, www.r-project.org/; genomic SEM v0.0.5 (including our new Q_{SNP} extension), https://github.com/genomicsem/genomicsem; METAL release 2020-05-05, https://genome.sph.umich.edu/wiki/metal; FUMA GWAS v.1.5.2, https://fuma.ctglab.nl; SMR v.1.3.2, https://yanglab.westlake.edu.cn/software/smr/; METASCAPE v.3.5.20250101, https://metascape.org/gp/index.html#/main/step1; lavaan R package v.0.6-19, https://lavaan.ugent.be/; MungeSumstats R package v.1.14.1, https://github.com/neurogenomics/mungesumstats; MAGMA v.1.08, https://cncr.nl/research/magma/; stats R package v.4.4.2, https://stat.ethz.ch/R-manual/R-devel/library/stats/html/00Index.html; and SBayesR v.2.0, https://cnsgenomics.com/software/gctb/#Overview. The specific custom code for the analyses in this study is publicly available via GitHub at https://github.com/IsyFoote/Frailty-Multivariate-GWAS and Zenodo at https://doi.org/10.5281/zenodo.15654248 (ref. 104). The code used to create the latent growth curve models of cognitive ability and cognitive change in LBC1936 can be found at https://lothianbirthcohorts.github.io/longitudinal-g-models/longitudinal_g_models.

References

51. Sepehri, K. et al. A computerized frailty assessment tool at points-of-care: development of a standalone electronic Comprehensive Geriatric Assessment/Frailty Index (eFI-CGA). *Front. Public Health* **8**, 89 (2020).
52. Howard, D. M. et al. Genome-wide meta-analysis of depression identifies 102 independent variants and highlights the importance of the prefrontal brain regions. *Nat. Neurosci.* **22**, 343–352 (2019).
53. Purves, K. L. et al. A major role for common genetic variation in anxiety disorders. *Mol. Psychiatry* **25**, 3292–3303 (2020).
54. Wang, H. et al. Genome-wide association analysis of self-reported daytime sleepiness identifies 42 loci that suggest biological subtypes. *Nat. Commun.* **10**, 3503 (2019).
55. Trajanoska, K. et al. Genetic basis of falling risk susceptibility in the UK Biobank Study. *Commun. Biol.* **3**, 543 (2020).
56. Kemp, J. P. et al. Identification of 153 new loci associated with heel bone mineral density and functional involvement of GPC6 in osteoporosis. *Nat. Genet.* **49**, 1468–1475 (2017).
57. Bonfiglio, F. et al. GWAS of stool frequency provides insights into gastrointestinal motility and irritable bowel syndrome. *Cell Genom.* **1**, 100069 (2021).
58. Kaiser, H. F. The application of electronic computers to factor analysis. *Educ. Psychol. Meas.* **20**, 141–151 (1960).
59. Ruscio, J. & Roche, B. Determining the number of factors to retain in an exploratory factor analysis using comparison data of known factorial structure. *Psychol. Assess.* **24**, 282–292 (2012).
60. Ximénez, C., Revuelta, J. & Castañeda, R. What are the consequences of ignoring cross-loadings in bifactor models? A simulation study assessing parameter recovery and sensitivity of goodness-of-fit indices. *Front. Psychol.* **13**, 923877 (2022).
61. Eid, M., Krumm, S., Koch, T. & Schulze, J. Bifactor models for predicting criteria by general and specific factors: problems of nonidentifiability and alternative solutions. *J. Intell.* **6**, 42 (2018).
62. Kunkle, B. W. et al. Genetic meta-analysis of diagnosed Alzheimer's disease identifies new risk loci and implicates Aβ, tau, immunity and lipid processing. *Nat. Genet.* **51**, 414–430 (2019).
63. Nalls, M. A. et al. Identification of novel risk loci, causal insights, and heritable risk for Parkinson's disease: a meta-analysis of genome-wide association studies. *Lancet Neurol.* **18**, 1091–1102 (2019).
64. van Rheenen, W. et al. Common and rare variant association analyses in amyotrophic lateral sclerosis identify 15 risk loci with distinct genetic architectures and neuron-specific biology. *Nat. Genet.* **53**, 1636–1648 (2021).
65. Persyn, E. et al. Genome-wide association study of MRI markers of cerebral small vessel disease in 42,310 participants. *Nat. Commun.* **11**, 2175 (2020).
66. Bell, S., Tozer, D. J. & Markus, H. S. Genome-wide association study of the human brain functional connectome reveals strong vascular component underlying global network efficiency. *Sci. Rep.* **12**, 14938 (2022).
67. Kaufmann, T. et al. Common brain disorders are associated with heritable patterns of apparent aging of the brain. *Nat. Neurosci.* **22**, 1617–1623 (2019).

68. Fürtjes, A. E. et al. General dimensions of human brain morphometry inferred from genome-wide association data. *Hum. Brain Mapp.* **44**, 3311–3323 (2023).
69. Wainberg, M. et al. Genetic architecture of the structural connectome. *Nat. Commun.* **15**, 1962 (2024).
70. Traylor, M. et al. Genetic basis of lacunar stroke: a pooled analysis of individual patient data and genome-wide association studies. *Lancet Neurol.* **20**, 351–361 (2021).
71. Mishra, A. et al. Stroke genetics informs drug discovery and risk prediction across ancestries. *Nature* **611**, 115–123 (2022).
72. Timmers, P. R. et al. Genomics of 1 million parent lifespans implicates novel pathways and common diseases and distinguishes survival chances. *eLife* **8**, e39856 (2019).
73. Deelen, J. et al. A meta-analysis of genome-wide association studies identifies multiple longevity genes. *Nat. Commun.* **10**, 3669 (2019).
74. Nethander, M. et al. Assessment of the genetic and clinical determinants of hip fracture risk: genome-wide association and Mendelian randomization study. *Cell Rep. Med.* **3**, 100776 (2022).
75. Butler-Laporte, G. et al. Increasing serum iron levels and their role in the risk of infectious diseases: a Mendelian randomization approach. *Int. J. Epidemiol.* **52**, 1163–1174 (2023).
76. Levin, M. G. et al. Genome-wide association and multi-trait analyses characterize the common genetic architecture of heart failure. *Nat. Commun.* **13**, 6914 (2022).
77. Pathak, G. A. et al. A first update on mapping the human genetic architecture of COVID-19. *Nature* **608**, E1–E10 (2022).
78. Said, S. et al. Genetic analysis of over half a million people characterises C-reactive protein loci. *Nat. Commun.* **13**, 2198 (2022).
79. Stanzick, K. J. et al. Discovery and prioritization of variants and genes for kidney function in >1.2 million individuals. *Nat. Commun.* **12**, 4350 (2021).
80. Lagou, V. et al. GWAS of random glucose in 476,326 individuals provide insights into diabetes pathophysiology, complications and treatment stratification. *Nat. Genet.* **55**, 1448–1461 (2023).
81. Bell, S. et al. A genome-wide meta-analysis yields 46 new loci associating with biomarkers of iron homeostasis. *Commun. Biol.* **4**, 156 (2021).
82. Mallard, T. T. et al. Multivariate GWAS of psychiatric disorders and their cardinal symptoms reveal two dimensions of cross-cutting genetic liabilities. *Cell Genom.* **2**, 100140 (2022).
83. Watanabe, K., Taskesen, E., van Bochoven, A. & Posthuma, D. Functional mapping and annotation of genetic associations with FUMA. *Nat. Commun.* **8**, 1826 (2017).
84. Grotzinger, A. D. et al. Genetic architecture of 11 major psychiatric disorders at biobehavioral, functional genomic and molecular genetic levels of analysis. *Nat. Genet.* **54**, 548–559 (2022).
85. Finucane, H. K. et al. Partitioning heritability by functional annotation using genome-wide association summary statistics. *Nat. Genet.* **47**, 1228–1235 (2015).
86. Ardlie, K. G. et al. The Genotype-Tissue Expression (GTEx) pilot analysis: multitissue gene regulation in humans. *Science* **348**, 648–660 (2015).
87. Pers, T. H. et al. Biological interpretation of genome-wide association studies using predicted gene functions. *Nat. Commun.* **6**, 5890 (2015).
88. Kundaje, A. et al. Integrative analysis of 111 reference human epigenomes. *Nature* **518**, 317–330 (2015).
89. Karczewski, K. J. et al. The mutational constraint spectrum quantified from variation in 141,456 humans. *Nature* **581**, 434–443 (2020).
90. Grotzinger, A. D. et al. Multivariate genomic architecture of cortical thickness and surface area at multiple levels of analysis. *Nat. Commun.* **14**, 946 (2023).
91. Grotzinger, A. D., de la Fuente, J., Davies, G., Nivard, M. G. & Tucker-Drob, E. M. Transcriptome-wide and stratified genomic structural equation modeling identify neurobiological pathways shared across diverse cognitive traits. *Nat. Commun.* **13**, 6280 (2022).
92. de Leeuw, C. A., Mooij, J. M., Heskes, T. & Posthuma, D. MAGMA: generalized gene-set analysis of GWAS data. *PLoS Comput. Biol.* **11**, e1004219 (2015).
93. Aguet, F. et al. The GTEx Consortium atlas of genetic regulatory effects across human tissues. *Science* **369**, 1318–1330 (2020).
94. de Leeuw, C. A., Stringer, S., Dekkers, I. A., Heskes, T. & Posthuma, D. Conditional and interaction gene-set analysis reveals novel functional pathways for blood pressure. *Nat. Commun.* **9**, 3768 (2018).
95. Zhu, Z. et al. Integration of summary data from GWAS and eQTL studies predicts complex trait gene targets. *Nat. Genet.* **48**, 481–487 (2016).
96. Wu, Y. et al. Integrative analysis of omics summary data reveals putative mechanisms underlying complex traits. *Nat. Commun.* **9**, 918 (2018).
97. Lloyd-Jones, L. R. et al. Improved polygenic prediction by Bayesian multiple regression on summary statistics. *Nat. Commun.* **10**, 5086 (2019).
98. Choi, S. W., Mak, T. S.-H. & O'Reilly, P. F. Tutorial: a guide to performing polygenic risk score analyses. *Nat. Protoc.* **15**, 2759–2772 (2020).
99. Krapohl, E. et al. Multi-polygenic score approach to trait prediction. *Mol. Psychiatry* **23**, 1368–1374 (2018).
100. Jung, H. et al. Integration of risk factor polygenic risk score with disease polygenic risk score for disease prediction. *Commun. Biol.* **7**, 180 (2024).
101. Pain, O. et al. Evaluation of polygenic prediction methodology within a reference-standardized framework. *PLoS Genet.* **17**, e1009021 (2021).
102. Dickson, S. P. et al. GenoRisk: a polygenic risk score for Alzheimer's disease. *Alzheimers Dement.* **7**, e12211 (2021).
103. Flint, J. P. et al. Multi-polygenic prediction of frailty highlights chronic pain and educational attainment as key risk and protective factors. Preprint at *medRxiv* https://doi.org/10.1101/2024.05.31.24308260 (2024).
104. Foote, I. Frailty-multivariate-GWAS: release for Zenodo. *Zenodo* https://doi.org/10.5281/zenodo.15654248 (2025).

Acknowledgements

This study was facilitated by the Deep Dementia Phenotyping (DEMON) Network through the Frailty and Dementia Special Interest Group and is an outcome of a workshop entitled 'Frailty and Precision Dementia Medicine' funded by the University of Exeter Global Partnerships Fund (J.M.R.). This work was funded by grants from the National Institute on Aging (I.F.F., A.E.F. and A.D.G., grant no. R01AG073593) and the National Institute of Mental Health (A.D.G. and J.M.L., grant no. R01MH120219). The DEMON Network is supported by Alzheimer's Research UK (D.J.L. and J.M.R.). D.J.L. is also supported by the National Institute for Health and Care Research Applied Research Collaboration South West Peninsula. The LBC1936 is supported by the Biotechnology and Biological Sciences Research Council, the Economic and Social Research Council (no. BB/W008793/1), Age UK (The Disconnected Mind Project), the Milton Damerel Trust and The University of Edinburgh. S.R.C. is supported by a Sir Henry Dale Fellowship jointly funded by the Wellcome Trust and the Royal Society (no. 221890/Z/20/Z). ELSA is funded by the National Institute on Aging (grant no. R01AG017644) and by UK Government Departments coordinated by the National Institute for Health and Care Research. PISA is funded by the National Health and Medical Research Council (grant no. APP1095227). J.P.F. is funded by the Legal & General Group (research grant to establish the independent Advanced Care Research Centre at the University of Edinburgh). Legal & General had no role in

the conduct of the study, its interpretation or the decision to submit for publication; the views expressed are those of the authors and not necessarily those of Legal & General. J.D.F. receives research grant support from the Canadian Institutes of Health Research, the National Multiple Sclerosis Society and MS Canada, and consultation and distribution royalties from the MAPI Research Trust. A.R. thanks the Natural Sciences and Engineering Research Council of Canada for operating grant no. RGPIN-2019-05888. K.R. is supported by Dalhousie University Faculty of Medicine Advancement funding as Clinical Research Professor of Frailty and Aging. We thank the authors of the original GWAS publications we used in this study for making their data publicly available, including the Pan-UK Biobank team and FinnGen (for unpublished, freely available GWAS data from the UK Biobank and FinnGen). We also thank the participants of the contributing cohorts for providing their data for this work.

Author contributions

I.F.F., A.D.G., J.D.F., A.R., J.M.R., D.J.L., T.K.K. and K.R. conceived the study. I.F.F., J.P.F., A.E.F. and J.M.L. performed the analyses. S.R.C., M.L., N.G.M. and M.K.L. provided key data access and support for the study analyses. J.P.F. and D.S.M. performed the data curation of phenotypes in the external individual-level datasets. I.F.F., A.D.G. and J.P.F. wrote the initial manuscript. All authors contributed to the design and conceptual aspects of the study and critically reviewed the final manuscript.

Competing interests

Although not directly related to the submitted work, K.R. has asserted copyright over the Clinical Frailty Scale and (with O. Theou) the Pictorial Fit-Frail Scale, which have been made freely available for noncommercial education and research, and nonprofit healthcare via completion of a permission agreement stipulating that users will not change, charge for or commercialize the scales. For-profit entities (including pharma) pay a licensing fee, 15% of which is retained by the Dalhousie University Office of Commercialization and Industry Engagement. After taxes, the remainder of the license fees are donated to the Dalhousie Medical Research Foundation. In the past 3 years, licenses have been negotiated with Renibus Therapeutics, Cook Research Incorporated, W.L. Gore Associates, Pfizer, Cellcolabs AB, AstraZeneca UK, Qu Biologics, Biotest AG, BioAge Labs, Congenica and Icosavax. The other authors declare no competing interests.

Additional information

Supplementary information The online version contains supplementary material available at https://doi.org/10.1038/s41588-025-02269-0.

Correspondence and requests for materials should be addressed to Isabelle F. Foote.

Peer review information *Nature Genetics* thanks Fernando Rivadeneira and Sarah Gagliano Taliun for their contribution to the peer review of this work. Peer reviewer reports are available.

nature portfolio

Corresponding author(s): Isabelle F. Foote

Last updated by author(s): Jun 13, 2025

Reporting Summary

Nature Portfolio wishes to improve the reproducibility of the work that we publish. This form provides structure for consistency and transparency in reporting. For further information on Nature Portfolio policies, see our Editorial Policies and the Editorial Policy Checklist.

Statistics

For all statistical analyses, confirm that the following items are present in the figure legend, table legend, main text, or Methods section.

n/a	Confirmed
☐	☒ The exact sample size (*n*) for each experimental group/condition, given as a discrete number and unit of measurement
☐	☒ A statement on whether measurements were taken from distinct samples or whether the same sample was measured repeatedly
☐	☒ The statistical test(s) used AND whether they are one- or two-sided *Only common tests should be described solely by name; describe more complex techniques in the Methods section.*
☐	☒ A description of all covariates tested
☐	☒ A description of any assumptions or corrections, such as tests of normality and adjustment for multiple comparisons
☐	☒ A full description of the statistical parameters including central tendency (e.g. means) or other basic estimates (e.g. regression coefficient) AND variation (e.g. standard deviation) or associated estimates of uncertainty (e.g. confidence intervals)
☐	☒ For null hypothesis testing, the test statistic (e.g. *F*, *t*, *r*) with confidence intervals, effect sizes, degrees of freedom and *P* value noted *Give P values as exact values whenever suitable.*
☒	☐ For Bayesian analysis, information on the choice of priors and Markov chain Monte Carlo settings
☐	☒ For hierarchical and complex designs, identification of the appropriate level for tests and full reporting of outcomes
☐	☒ Estimates of effect sizes (e.g. Cohen's *d*, Pearson's *r*), indicating how they were calculated

Our web collection on statistics for biologists contains articles on many of the points above.

Software and code

Policy information about availability of computer code

Data collection	No data collection was completed for this study.
Data analysis	This code was developed using publicly available software that is available via the following links: R v4.4.2 Genomic SEM v0.0.5 (including our new QSNP extension) METAL v released on 2020-05-05 FUMA v1.5.2 SMR v1.3.2 METASCAPE v3.5.20250101 lavaan R package v0.6-19 MungeSumstats R package v1.14.1 MAGMA v1.08 stats R package v4.4.2 SBayesR v2.0 The specific custom code for the analyses in this study are publicly available at https://github.com/IsyFoote/Frailty-Multivariate-GWAS and Zenodo 10.5281/zenodo.15654248. The code we used to create the latent growth curve models of cognitive ability and cognitive change in LBC1936 can be found here.

For manuscripts utilizing custom algorithms or software that are central to the research but not yet described in published literature, software must be made available to editors and reviewers. We strongly encourage code deposition in a community repository (e.g. GitHub). See the Nature Portfolio guidelines for submitting code & software for further information.

Data

Policy information about availability of data

All manuscripts must include a data availability statement. This statement should provide the following information, where applicable:

- Accession codes, unique identifiers, or web links for publicly available datasets
- A description of any restrictions on data availability
- For clinical datasets or third party data, please ensure that the statement adheres to our policy

The latent frailty factor and pneumonia GWAS summary statistics that were created in this study are available on GWAS Catalog (accession codes GCST90624046-GCST90624053). The frailty PRS created in this study are available on PGS Catalog (IDs PGS005221-PGS005229). Individual-level data that was used for our polygenic risk score analyses can be accessed upon request from the relevant cohorts: LBC1936, PISA and ELSA.

The univariate GWAS summary statistics that we used for our frailty model and the external health outcomes are available via the citations outlined in Supplementary Tables 1 and 4, respectively. The LD scores and weights, HapMap3 SNPs and 1000 Genomes reference file for Genomic SEM are available to download here (https://utexas.app.box.com/s/vkd36n197m8klbaio3yzoxsee6sxo11v) and the functional annotations for conducting Stratified Genomic SEM are available to download here (https://github.com/GenomicSEM/GenomicSEM/wiki/6.-Stratified-Genomic-SEM). The datasets used for positional, eQTL and chromatin interaction mapping and MAGMA analyses are available on the online platform FUMA (https://fuma.ctglab.nl), and the pre-processed eTL, sQTL and mQTL data for conducting SMR are available for download here (https://yanglab.westlake.edu.cn/software/smr/#DataResource). The databases used for pathway analysis are available via the online platform METASCAPE (https://metascape.org/gp/index.html#/main/step1).

Research involving human participants, their data, or biological material

Policy information about studies with human participants or human data. See also policy information about sex, gender (identity/presentation), and sexual orientation and race, ethnicity and racism.

Reporting on sex and gender	We use the term sex in our current study, which is determined by the composition of sex chromosomes in the individuals within our sample. We did this for everyone by confirming that their sex according to their genetic data matched their self-reported sex (i.e. males should have chromosome composition of X/Y and females should have X/X composition). This was done based on heterozygosity on the X chromosome and whether the individual displayed genotyping on the Y chromosome. Sample mismatches were re-classified in line with their genetically determined biological sex where possible, or were removed from the analysis. In addition, participants that displayed chromosomal aneuploidy (e.g. X/O females or X/X/Y males) were excluded from our analyses. None of our analyses were stratified by sex but we provide the ratio of male and female individuals within our cohort samples that we used for polygenic risk prediction in the Supplementary Methods.
Reporting on race, ethnicity, or other socially relevant groupings	wing to the restrictions of the methods used in our study and the lack of data available currently for analysis of non-European samples, we restricted our current analysis to samples that included individuals that were predominantly of European ancestry (confirmed using methods such a principal component analysis).
Population characteristics	Population characteristics for the 30 included GWAS studies in our frailty model are outlined in the main text, Supplementary Note and Supplementary Tables 1 and 4. They were measured within the European ancestry samples collected by consortia, biobank studies and cohort studies. For the individual-level analyses in the 3 external cohorts the population characteristics are outlined in detail in the Supplementary Note. For LBC1936 wave 1 the mean age was 69.90 (SD= 0.83); for ELSA the mean age was 68.45 (SD= 10.13); and for PISA the mean age was 60.34 (SD= 6.98).
Recruitment	We did not complete any new recruitment for the current study.
Ethics oversight	Ethics for LBC1936 was approved by the Multi-Centre Research Ethics Committee for Scotland (Wave 1: MREC/01/0/56), the Lothian Research Ethics Committee (Wave 1: LREC/2003/2/29), and the Scotland A Research Ethics Committee (Waves 2, 3, 4 and 5: 07 /MRE00/58) and all methods were performed in accordance with the relevant guidelines and regulations. Informed Written Consent was obtained from participants at each of the waves. Ethical approval for ELSA was gained via the South Central - Berkshire Research Ethics Committee (21/SC/0030, 22nd March 2021) and all methods were performed in accordance with the relevant guidelines and regulations. The ELSA genetics team approved a request for this study to utilize raw genotypes and provided linked genome-wide association study (GWAS) data to the phenotypic data curated at the Advanced Care Research Centre, University of Edinburgh. The PISA study protocol was approved by the Human Research Ethics Committee (HREC) at QIMR Berghofer Medical Research Institute. The remaining data used in this study represents publicly available, anonymised, summary-level data that did not require specific ethical approval to be used in our analyses.

Note that full information on the approval of the study protocol must also be provided in the manuscript.

Field-specific reporting

Please select the one below that is the best fit for your research. If you are not sure, read the appropriate sections before making your selection.

☒ Life sciences ☐ Behavioural & social sciences ☐ Ecological, evolutionary & environmental sciences

For a reference copy of the document with all sections, see nature.com/documents/nr-reporting-summary-flat.pdf

Life sciences study design

All studies must disclose on these points even when the disclosure is negative.

Sample size	No power calculations were calculated but we only included phenotypes in our main analysis that demonstrated a strong heritable component (SNP-based h2 Z statistic> 4), which indicates that the phenotype has enough power to be reliably included within Genomic SEM analyses. Furthermore, we only used GWAS summary statistics that had sample sizes >10,000 individuals. Sample sizes of the GWAS summary statistics that formed our latent model are detailed in our Supplementary Tables 1 and 4, but constitute the largest, publicly available univariate GWAS sample for each phenotype to maximise power in our multivariate analysis. These strategies ensured that we followed the best practice guidance on performing well-powered Genomic SEM analyses since each univariate trait had already either had power calculations performed by the relevant consortium or was given high confidence status by the PanUKB team in their QC analyses (as described here: https://pan.ukbb.broadinstitute.org/docs/per-phenotype-files). The expected sample size for each of the latent factor GWAS phenotypes that we estimated was calculated using standard methods and is outlined in the methods section and in the results of our paper. Sample sizes, including descriptive of age and sex, for the 3 external cohort datasets that we used for polygenic risk score estimation (LBC 1936, ELSA and PISA) are outlined in detail in our Supplementary Methods and in our results sections. For LBC 1936 the sample size was 1,005 individuals, for ELSA it was 7,181 individuals and for PISA it was 3,265 individuals.
Data exclusions	Owing to a reliance on linkage disequilibrium information for the methods used here, we excluded participants of non-European ancestry as we did not have sufficient data available to conduct our analyses reliably in non-European ancestry populations. We also excluded genotyped and imputed SNPs with a minor allele frequency <1% and an imputation score <0.9 (for LDSC analyses) and <0.6 for our multivariate GWAS analysis, in line with the standard recommendations for these methods.
Replication	Since there were not separate samples large enough to fully replicate all 30 GWAS traits in our main analysis, we conducted exploratory factor analysis in the odd autosomes and confirmatory factor analysis in the even autosomes to minimise overfitting our model. We performed our polygenic risk score analyses in 3 external datasets that were not overlapping with our GWAS summary statistics from which the risk scores were estimated.
Randomization	Not relevant to this study as it was not a clinical trial study and all data was from observational studies.
Blinding	Blinding was not relevant to the current study because the study utilised summary data and observational analytical methods that did not require the researcher to provide an intervention to participants at any point.

Reporting for specific materials, systems and methods

We require information from authors about some types of materials, experimental systems and methods used in many studies. Here, indicate whether each material, system or method listed is relevant to your study. If you are not sure if a list item applies to your research, read the appropriate section before selecting a response.

Materials & experimental systems

n/a	Involved in the study
☒	☐ Antibodies
☒	☐ Eukaryotic cell lines
☒	☐ Palaeontology and archaeology
☒	☐ Animals and other organisms
☒	☐ Clinical data
☒	☐ Dual use research of concern
☒	☐ Plants

Methods

n/a	Involved in the study
☒	☐ ChIP-seq
☒	☐ Flow cytometry
☒	☐ MRI-based neuroimaging

Plants

Seed stocks	N/A
Novel plant genotypes	N/A
Authentication	N/A